Wiley
Journal of Renewable Energy
Volume 2024, Article ID 1343256, 31 pages
https://doi.org/10.1155/2024/1343256

WILEY

Review Article

Understanding the Factors Influencing the Properties of Biomass-Derived Porous Carbon and Their Impacts on Electrical Double-Layer Capacitor Electrodes: A Comprehensive Review

Colette Abimana,[1,2] **Abdulhakeem Bello**,[3,4] **Revocatus Machunda**,[1] **and Yusufu Abeid Chande Jande**[1]

[1]*Department of Materials Science and Engineering, School of Materials, Energy, Water, and Environmental Sciences, Nelson Mandela African Institution of Science and Technology, P.O. Box 447, Arusha, Tanzania*
[2]*Department of Physics, School of Science, College of Science and Technology, University of Rwanda, P.O. Box 3900, Kigali, Rwanda*
[3]*Department of Theoretical and Applied Physics, African University of Science and Technology, Abuja 900107, Nigeria*
[4]*Centre for Cyber-Physical Food, Energy & Water Systems (CCP-FEWS), University of Johannesburg, Johannesburg 2006, South Africa*

Correspondence should be addressed to Colette Abimana; c.abimana@ur.ac.rw and Yusufu Abeid Chande Jande; yusufu.jande@nm-aist.ac.tz

Received 22 October 2023; Revised 3 August 2024; Accepted 8 August 2024

Academic Editor: Prakash Bhuyar

The use of biomass as carbon precursors has been extensively investigated, with a particular emphasis on examining the properties of derived porous carbon and its application in electrical double-layer capacitors (EDLCs). Biomass-derived porous carbon-based electrodes have shown promising properties that can improve the efficiency of EDLCs. However, despite the extensive research in this field, no definitive solution has been proposed. This review investigates in depth three main factors that impact the electrochemical performance of derived porous carbon-based electrodes: (1) the initial properties of raw biomass as carbon precursors, (2) operating conditions, and (3) physicochemical properties of biomass-derived porous carbon materials. Examined operating conditions include synthesis techniques, activating agents, the mass ratio of the activating agent to the raw biomass as porous carbon precursors, carbonization/activation duration, operating temperature, and the mass of the active material in the electrode. The surface morphology and surface functional groups were used to evaluate the physicochemical properties of derived porous carbon materials. Multiple factors influence the properties of porous carbon derived from biomass and, consequently, the efficiency of the electrodes made from these materials. This study reveals that the properties of porous carbon-based electrodes derived from biomass vary from one biomass to another and are affected by various parameters, conditions, and synthesis techniques. Therefore, it is impossible to rely exclusively on a single factor to improve the electrochemical performance of EDLC electrodes. A thorough consideration of the multiple factors is required to optimize the properties and performance of the electrodes.

1. Introduction

Because of the limited resources and environmental concerns associated with nonconventional energy resources, the global landscape has shifted towards renewable energy resources. The intermittent nature of renewables, however, poses challenges to their reliability and integration with primary energy sources, necessitating the development of high-capacity energy storage systems [1, 2]. This has led to the dominance of lithium-ion batteries, lead-acid batteries, and supercapacitors for solar and wind energy technologies. However, batteries

have limitations such as low power density, a slow charge rate, and a short lifetime [3]. Supercapacitors have emerged as promising candidates among these energy storage technologies due to their unique characteristics, including rapid charge/discharge, high power density, long life cycle, and stability [4, 5]. However, they have disadvantages such as high self-discharge and low-energy density [6–10]. Within the supercapacitor family, electric double-layer capacitors (EDLCs) have acquired widespread uses in many electronic devices, electric vehicles, and grid and off-grid connections [1, 2, 11]. Using an electrostatic adsorption/desorption mechanism for the charging/discharging process of EDLCs, these capacitors store energy by forming temporary electrical double layers of ions at the electrode-electrolyte interface. Consequently, the distance between electrodes decreases and leads to an increase in the capacitance [12].

The electrolyte must be considered when evaluating the electrochemical performance of an electrode as the charging/discharging process takes place at the interface between the electrode and electrolyte. There are three categories of electrolytes currently in use: solid, gel, and aqueous [13, 14]. Given the EDLC's charging/discharging mechanism, the electrode plays a crucial role in determining the performance of EDLCs [12, 15–21]. The overall performance of an EDLC depends on the electrochemical properties of the electrodes, which are influenced by the physicochemical properties of the materials used in the electrode fabrication as ions have to be accumulated on the surface of active materials within electrodes [22]. Therefore, the selection of carbon materials to be used must be done attentively. Electrode materials must possess appropriate physicochemical properties to produce EDLCs with high performance. Several essential properties are necessary to improve the efficiency of EDLCs. The properties include a large specific surface area (SSA) and pore size distribution that includes micro-, meso-, and macropores. Furthermore, optimal electrode performance requires high electrical conductivity, mechanical and chemical stability [19], desired surface functional groups [23, 24], and electrochemical stability [6]. The active material, high-conducting material, and binder constitute the electrode's materials. These materials are coated on a current collector to facilitate electrochemical performance measurement of an electrode in a three- or two-electrode cell with minimal risk of leakages [25–27]. Thus, the weight and capacitance of the active materials must be greater than that of the other electrode components [7, 21, 28]. Therefore, this report focuses on the active materials derived from the aforementioned constituents of electrode materials.

Carbonaceous materials such as activated carbon (AC), carbon nanotubes (CNTs) [7, 12, 16, 25, 29], and activated graphene [30] have shown promise in the search for suitable active electrode materials. Among these alternatives, AC has attracted significant interest due to its excellent physicochemical properties, which are essential for EDLC electrodes [7, 12, 16, 25, 29]. Extensive research in the past decade has identified AC derived from biomass as a promising candidate for the electrode active materials for EDLC electrodes. Biomass-derived carbon materials have shown excellent properties of conductivity, good electrochemical stability, good thermal stability, and a wide voltage window [5, 6, 31]. Furthermore, AC derived from biomass has a high level of porosity, making it environmentally friendly, and it has a high specific surface with a random pore size distribution that presents a variety of surface functional groups that led to electrodes with good electrochemical properties as well as performance [32–35] and a high carbon yield [29, 36–42]. As precursors for AC, biomass materials derived from various agricultural sources such as leaves, roots, trunks, shells, seeds, peels, husks, stalks, tassels, and grasses [4, 7, 17, 43–45] have been investigated. Various syntheses and conditions have been employed to produce the desired biomass-derived AC for specific applications. However, given that their uniqueness in thermal stability, chemical compositions, and surface chemistry vary from one biomass to the other, to the best of our knowledge there is no single recommended reliable synthesis method or perfect biomass-derived AC-based electrode materials yet found.

So far, several reviews have been conducted on biomass-derived carbon materials. These include evaluations of the synthesis and performance of various biomass-derived carbon-based electrodes for EDLC application [46–49]; the influence of synthesis conditions on physical and chemical behaviors of biomass-derived carbon-based electrodes [50]; progress in the synthesis of biomass-derived carbon and the relationship between the surface morphology, chemical compositions, and electrochemical properties [51–53]; examination of how synthesis methods and conditions affect the morphology and valence state elements in biomass-derived carbon [54]; future direction and challenges in biomass-based supercapacitors [55]; and many reviews focused on the synthesis of biomass-derived carbon and their application as electrode's materials for EDLC [25, 53, 56, 57]. It is also important to note that the same type of biomass can vary considerably based on geographic location and agricultural practices. Thus, it requires a deep investigation to address the impact of these variability on the performance and consistency of the electrode materials [25, 53, 56, 57]. Nonetheless, there is a dearth of available reviews on the topic under consideration.

This review investigates the impact of the initial properties of raw biomass as carbon precursor, various synthesis techniques, and the operating conditions on the physicochemical properties of AC derived from biomass. This impact extends to the electrochemical properties and performance of EDLC electrodes. The review makes a significant contribution to the understanding of how these factors influence the performance of EDLC electrodes by examining in detail how the AC is produced, the conditions under which it is produced, and the physicochemical properties. Furthermore, it provides valuable insights into the potential of AC derived from biomass as an ecofriendly and high-performance material for energy storage. Finally, it highlights the challenges associated with biomass utilization and identifies future research opportunities in this field.

2. Factors Affecting the Properties of Biomass-Derived Activated Carbon

The electrochemical performance of EDLCs is influenced by the physicochemical properties of electrode materials and electrolytes due to the charging and discharging mechanisms, which occur between electrodes' surface and ions from the electrolyte. The electrode is constituted of active materials that govern its properties, high-conducting materials to increase its conductivity, and binders to improve the adhesion of both materials to the current collector. In addition to the electrode materials and electrolyte, the efficiency of the system is also affected by the current collectors and separators [21]. It has been discovered that there is no single parameter that determines the capacitance of EDLC [58]. Therefore, the effect of different parameters and/or physicochemical properties, as well as the production process conditions, on the properties of EDLC was investigated. This section describes the effects of activation time [59], surface functional groups [23, 26, 60], pore size distribution [61], pore size, the ratio of carbon materials to the activation reagent, operation temperature [62–64], the mass of active material in the electrode, the thickness of the electrode [21], heating rate [63], the mass ratio of the activating agent to biomass raw materials [65], the activation method and type of activating agent [66], the density of electrode materials [67], and initial properties of the precursor [64]. These conditions and parameters can be classified into four categories: the initial properties of biomass as carbon precursors, operating conditions, physicochemical properties, and the mass of the active material and the thickness of the electrode.

2.1. The Effect of Initial Properties of Biomass as Carbon Precursors. As indicated in Tables 1 and 2, different biomasses synthesized under the same conditions result in carbon materials with different physicochemical properties and electrochemical performance. The initial chemical element composition of biomass influences the surface functional groups of resultant AC, which may contribute to the improvement of electronic conductivity, wettability, porosity, and interconnectivity of pores as well as increasing the SSA of derived AC materials, thereby enhancing the performance of the system [80, 81, 85, 89]. These elements play an important role in self-heteroatom doping [80] and the self-activation process [81, 90]. For example, laver's chemical composition contains nitrogen (N), oxygen (O), and sulphur (S), which improve pseudocapacitive performance and increase the accessibility of active sites for electrolyte ions, thereby improving the storage capacity of carbon-based materials [80]. While the self-activation of carbon derived from rotten potatoes has demonstrated a high SSA with a larger pore volume, larger average pore diameter, high electrical conductivity, and good specific capacitance (C_{SP}), this has led to a supercapacitor with excellent electrochemical performance and cycling stability. It was discovered that such properties resulted from the presence of the initial chemical elements potassium (K), calcium (Ca), sodium (Na), nitrogen (N), and oxygen (O) in decaying potatoes [81]. In the research conducted on the effect of precursors on the capacitive performance of electrodes from karagash and pine sawdust under similar conditions, the results showed that AC from karagash sawdust had a higher graphitization degree and capacitive performance with the lowest equivalence series resistance than AC from pine sawdust. However, the composition of the karagash sawdust-derived AC revealed the presence of K and Ca, which were absent in the pine-derived AC [64]. Their presence may contribute to the high-capacity performance of AC derived from karagash sawdust. As reported, these types of elements introduce defects into the carbon skeleton during activation, thereby increasing the porosity and specific surface area, which improves the electrochemical performance of porous carbon-based electrodes [85, 91–94]. Therefore, it is very important to select the right biomass materials to start with as AC precursors for producing AC with adequate properties required for EDLC electrodes.

2.2. Effect of Operating Conditions. Operating conditions include different methods used during the synthesis of raw materials and preparation of electrodes, and process parameters including temperature, activation agents, time of carbonization/activation, heating rate, the ratio of activating agent to raw biomass materials, and the ratio of the carbon content to the activating agent.

2.2.1. Synthesis Method of Biomass-Derived Activated Carbon and Activating Agent. Figure 1 shows that the synthesis of biomass-derived AC materials consists of three main steps: cleaning and impregnation of raw biomass materials used as carbon precursors, carbonizing and activating the carbon, and then washing the AC materials to remove impurities. The selection of the synthesis method has a significant effect on the morphological structure and properties of the carbon materials produced [54, 95, 96]. In addition, the synthesis conditions are highly dependent on the physical and chemical properties of raw biomass [54]. The synthesis of AC from biomass involves two processes: carbonization and activation, which can be performed in single-phase or two-phase processes. Carbonization and activation occur simultaneously in a single-phase process, while in a two-phase process, carbonization takes place first, followed by the activation process [12, 62]. The carbonization process is a process that uses heat to transform biomass materials into intense and cleansed carbon materials [97, 98]. That produced carbon can be called biochar or hydrochar depending on the employed carbonization technique, while the activation process is a heat-assisted process of modifying properties of carbon by introducing/removing chemical functional groups and increasing the degree of porosity with the final product, which is known as activated carbon [99, 100].

Several techniques, such as pyrolysis, hydrothermal carbonization, gasification [101], and pyrolytic templating synthesis [57, 102, 103], have been utilized for the synthesis

Table 1: Physicochemical properties of different biomass-derived activated carbon-based electrodes synthesized through different methods under different conditions.

Type of biomass	Activation reagent/solvent	Temperature (°C)	Specific surface area ($m^2 \cdot g^{-1}$)	Pore size (nm)	C (%)	O (%)	N (%)	B (%)	P (%)	S (%)	I_D/I_G	Specific capacitance (Fg^{-1})	Reference
Walnut shells	$KCl^{(ca)}$	900	1958	2.30	NR	NR	NR	NR	NR	NR	1.20	245	[59]
Corncob	$KOH^{(ca)}$	850	3054	0.5–4	89.45	9.49	<0.3	NR	NR	NR	NR	401.6	[4]
Banana peels	$KOH^{(ca)}$	900	1362	NR	NR	NR	NR	NR	NR	NR	0.8	165	[68]
Datura metel peels	$KOH^{(ca)}$	800	818	1.8	59.48	37.22	NR	NR	NR	NR	0.85	76.4	[69]
European deciduous trees	HNO_3: $H_2SO_4{}^{(ca)}$	$500^{(p)}$ and 700	614	3.4	84.12	11.19	NR	NR	NR	NR	1.08	236	[70]
Willow catkin	$KOH^{(ca)}$	600	645	0.77	74.63	13.28	2.51	NR	NR	NR	0.79	340	[71]
Pine cones	$KOH^{(ca)}$	$160^{(hc)}$ and 800	1515	1–100	NR	NR	NR	NR	NR	NR	0.99	137	[32]
Cotton fiber	$Mg(NO_3)_2{}^{(tm)}$ and $ZnCl_2{}^{(ca)}$	800	1990	NR	NR	NR	NR	NR	NR	NR	1.059	240	[72]
Banana peels	Ethanol and deionized water	$200^{(hc)}$	294.6	7.71	80.46	15.67	NR	NR	NR	NR	0.84	199	[73]
Succulent leaves	$Mg(NO_3)_2.6H_2O$ and $ZnCl_2{}^{(ca)}$ and $CH_4N_2S^{(d)}$	800	2136.2		81.49	6.8	9.5	NR	NR	2.21	1.05	455.3	[74]
Foxtail grass seeds	$NaHCO_3$ and $KHCO_3{}^{(ca)}$	600	819	2.23	78.52	18.4	0.54	NR	NR	2.52	NR	358	[75]
Peach gum	KCl and 0.1MMn $(CH_3COO)_2{}^{(ca)}$ and $(NH_4)_2HPO_4{}^{(d)}$	700	1635	NR	79.04	12.59	6.84	NR	1.53	NR	0.86	490	[76]
Brinjal	$KOH^{(ca)}$ and $urea^{(d)}$	700	850	NR	NR	NR	NR	NR NR	NR	NR	0.85	466	[77]
Ginger	NaCl and $KCl^{(ca)}$ and $CH_4N_2S^{(d)}$	$450^{(p)}$ and $800^{(ca)}$	720	NR	NR	NR	NR	NR	NR	NR	0.92	456	[78]
Fir bark	$NH_4B_5O_8.4H_2O^{(d)}$	$180^{(hc)}$ and 800	955	0.96	71.14	6.30	9.74	12.77	NR	NR	NR	188	[79]
Laver	$ZnCl_2$ and $KCl^{(ca)}$ and $H_3BO_3{}^{(d)}$	800	1514.3	NR	75.81	12.55	6.33	4.41	NR	0.48	0.93	382.5	[80]
Rotten potatoes	Self-doped	$900^{(pa)}$	2201	2.74	94.35	4.35	1.30	NR	NR	NR	0.68	220	[81]
Lotus seed shells	$C_6H_6Na_{12}O_{24}P_6{}^{(tm)}$ and $NaOH^{(ca)}$	450 | and 650	3188	2–60	NR	NR	3.1	NR	NR	NR	NR	286	[82]
Shorea robusta	H_3PO_4	$400^{(p)}$ and 700	1269.5	NR	NR	NR	NR	NR	NR	NR	1.1	136.3	[83]
	KOH	$400^{(p)}$ and 700	280.6	NR	NR	NR	NR	NR	NR	NR	1.1	42.2	[83]
	Na_2CO_3	$400^{(p)}$ and 700	58.9	NR	NR	NR	NR	NR	NR	NR	1.2	59.1	[83]
Clove stems	KCl	$160^{(hc)}$ and 850	1459	0.5–2	90.51	2.59	6.90	NR	NR	NR	NR	451	[84]
Waste green tea	KOH	$800^{(p)}$ and 800	1996	0.5–5.5	85.4	12.87	1.6	NR	NR	NR	0.872	397	[85]

Note. $^{(ca)}$Chemically activated; $^{(pa)}$physically activated; $^{(p)}$carbonized through pyrolysis; $^{(hc)}$carbonized through hydrothermal carbonization; $^{(d)}$dopant source; $^{(tm)}$template method was involved, and NR means not reported.

Table 2: Electrochemical performance of different biomass-derived activated carbon-based electrodes synthesized through different techniques.

Type of biomass	Activation reagent/solvent	SSA ($m^2 \cdot g^{-1}$)	Current density (Ag^{-1})	Specific capacitance (Fg^{-1})	Energy density ($Whkg^{-1}$)	Power density (Wkg^{-1})	Cyclic stability (cycles)	Capacitance retention (%)	Equivalence series resistance (Ω)	Reference
Walnut shells	$KCl^{(ca)}$	1958	0.1–5	245	NR	NR	4000	95.4	1.7	[59]
Corncob	$KOH^{(ca)}$	3054	0.5–5	401.6	NR	NR	10000	100	0.8	[4]
Banana peels	$KOH^{(ca)}$	1362	0.5–5	165	18.6	485	10000	100	4.13	[68]
Datura metel peels	$KOH^{(ca)}$	818	NR	76.4	6.79	24450	NR	56.8	10	[69]
European deciduous trees	HNO_3: $H_2SO_4{}^{(ca)}$	614	0.25	24	0.53	51	10000	100	3.8	[70]
Custard apple	$KOH^{(ca)}$ $C_3H_6N_6{}^{(d)}$	1525	0.125–1	236	1.72	2825	10000	97–100	0.20	[86]
	$KOH^{(ca)}$ $H_2NCOONH_4{}^{(d)}$	1706	0.125–1	199	0.81	2245	10000		0.21	[86]
	$KOH^{(ca)}$ and $(NH_4)_2S_2O_8{}^{(d)}$	1042	0.125–1	290	0.42	1180	10000		0.24	[86]
Fig tree	$KOH^{(ca)}$ $C_3H_6N_6$	1575	0.125–1	283	1.23	2396	10000	97–100	0.25	[86]
	$KOH^{(ca)}$ $H_2NCOONH_4$	1669	0.125–1	280	0.79	1461	10000		0.51	[86]
	$KOH^{(ca)}$ and $(NH_4)_2S_2O_8$	1114	0.125–1	237	0.12	997	10000		0.55	[86]
Oliver tree	$KOH^{(ca)}$ and $C_3H_6N_6$	1400	0.125–1	225	0.92	2214	10000	97–100	0.29	[86]
	$KOH^{(ca)}$ and $H_2NCOONH_4$	1314	0.125–1	216	2.35	3039	10000		0.48	[86]
	$KOH^{(ca)}$ and $(NH_4)_2S_2O_8$	1075	0.125–1	312	1,82	2506	10000		0.22	[86]
Citrus bergamia peels	$H_3PO_4{}^{(ca)}$	NR	NR	142	47.4	240	5000	101	0.14	[87]
	$Mn_3(NO_4)_2{}^{(ca)}$	NR	0.1–1.5	284	50.8	240	5000	88	0.37	[87]
Willow catkin	$KOH^{(ca)}$	645	0.1–10	340	NR	NR	3000	92	<0.5	[71]
Pine cones	$KOH^{(ca)}$	1515	0.1–5	137	19	100	10000	100	1.5	[32]
Syzygium cumini	$CO_2{}^{(pa)}$		0.5–1	253	27.22	200	5000	96.5	1.2	[88]
Chrysopogon zizanioides root	$CO_2{}^{(pa)}$		0.5–1	294	16.72	200	5000	91.8	1.1	[88]
Cotton fiber	$Mg(NO_3)_2{}^{(tm)}$ and $ZnCl_2{}^{(ca)}$	1990	1–20	240	5.7	499.9	NR	71	6.7	[72]
Banana peels	Ethanol and deionized water	294.6	0.5–5	199	54.15	350	NR	29	1.6	[73]
Succulent leaves	$Mg(NO_3)_2.6H_2O$ and $ZnCl_2{}^{(ca)}$ and $CH_4N_2S^{(d)}$	2136.2	1–20	455.3	19.89	450	10000	87.3	1.05	[74]
Foxtail grass seeds	$NaHCO_3$ and $KHCO_3{}^{(ca)}$	819	0.5–2	358	18.2	NR	10000	91.2	0.8	[75]
Peach gum	KCl and 0.1MMn $(CH_3COO)_2{}^{(ca)}$ and $(NH_4)_2HPO_4{}^{(d)}$	1635	1-2	490	76.87	799.8	10000	89.9	0.31	[76]
Brinjal	$KOH^{(ca)}$ and $urea^{(d)}$	850	1–5	460	23	587	20000	83	NR	[77]
		850	1–5	466	61	9000	5000	77		[77]
Ginger	NaCl and $KCl^{(ca)}$ and $CH_4N_2S^{(d)}$	720	0.3–6	456	48.3	400	10000	95	6	[78]
Fir bark	$NH_4B_5O_8.4H_2O^{(d)}$	955	0.5–1	188	9.33	400	10000	91	0.33	[79]
Laver	$ZnCl_2$ and $KCl^{(ca)}$ and $H_3BO_3{}^{(d)}$	1514.3	1–20	382.5	NR	NR	NR	75.8	0.23	[80]
Rotten potatoes	Self-doped	2201	0.5	220	20.8	524	5000	100	NR	[81]

Table 2: Continued.

Type of biomass	Activation reagent/solvent	SSA ($m^2 \cdot g^{-1}$)	Current density (Ag^{-1})	Specific capacitance (Fg^{-1})	Energy density ($Whkg^{-1}$)	Power density (Wkg^{-1})	Cyclic stability (cycles)	Capacitance retention (%)	Equivalence series resistance (Ω)	Reference
Lotus seed shells	$C_6H_6Na_{12}O_{24}P_6$ [tm] and NaOH [ca]	3188	0.5	286	10.9	102600	7000	90	NR	[82]
Shorea robusta	H_3PO_4	1269.5	1–20	136.3	3	99.6	1000	96.9	0.4	[83]
	KOH	280.6	1–20	42.2	0.8	95.2	1000	89.5	0.5	[83]
	Na_2CO_3	58.9	1–20	59.1	1.82	95.1	1000	78.5	0.6	[83]
Clove stems	KCl	1459	0.5–20	451	10.7	125	10000	99.3	NR	[84]
Waste green tea	KOH	1996	0.005	397	142	630	50000	116	0.13	[85]

Note. [ca]Chemically activated; [pa]physically activated; [d]dopant source; [tm]template method was involved, and NR means not reported.

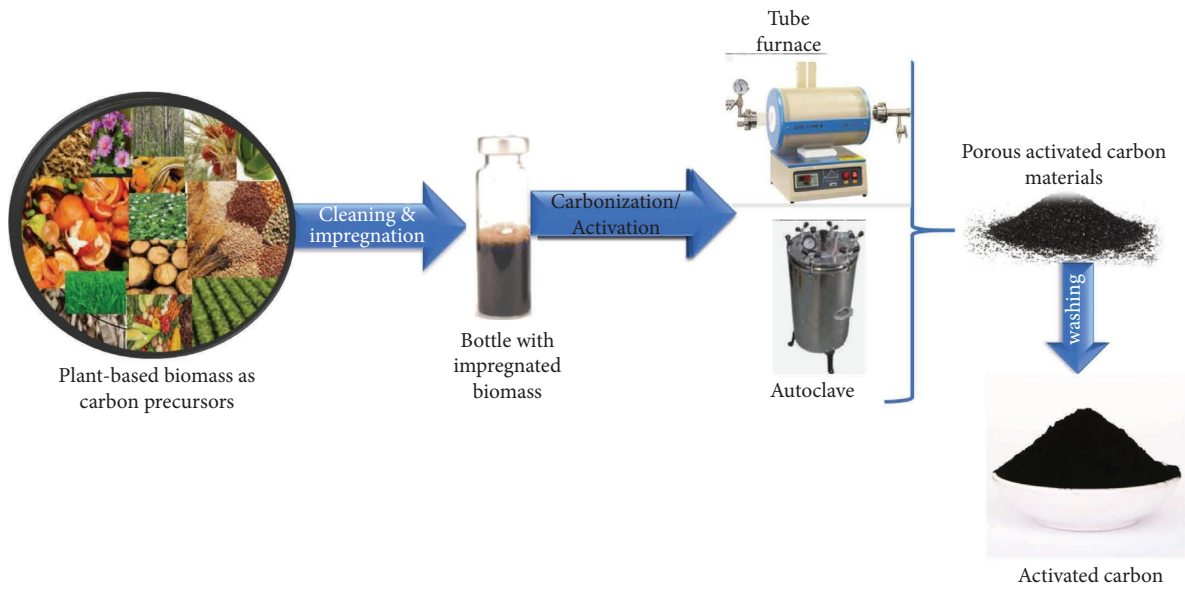

Figure 1: Schematic diagram of main procedures used in synthesizing biomass-derived porous carbon materials.

of carbon from biomass as precursors. Chemical activation and physical activation are widely recognized as the most popular activation methods in the production of AC. Activation is crucial; however, excessive activation may cause pore structure collapse, resulting in a decrease in SSA and degradation of the electrochemical performance of the AC [54]. The synthesis method used affects the properties of activated materials to be used in electrode fabrication. Different synthesis methods and activating agents will result in different properties [87, 104–107]. This study examined the effects of carbonization or preactivation methods, activation methods, doping, and templating techniques used to improve and modify the properties of carbon-based materials.

(1) Carbonization Techniques

(i) Hydrothermal Carbonization

Hydrothermal carbonization is a process that utilizes an aqueous solution as a solvent to which raw materials are added and heated in an autoclave or a hydrothermal reactor [95, 108]. This process is carried out at a relatively low temperature, 150–250°C, requiring minimal pretreatment of precursors and producing hydrochar [54]. Hydrothermal carbonization is regarded as a highly effective and environmentally friendly process that yields positive results [54, 109, 110]. The properties of hydrochar produced by hydrothermal carbonization are substantially influenced by variables such as the amount and composition of the solvent used, the operating temperature, and the carbonization time [111]. Hydrochars derived from hydrothermal carbonization possess a high carbon content, a low ash content, uniform structure properties [108], and a significant presence of surface oxygen groups [108, 112]. The presence of numerous functional groups in these hydrochars contributes to their enhanced cation exchange capacity, despite their low stability compared to biochars [95]. Due to the high concentration of oxygen functional groups on their surface, hydrochars typically exhibit a narrow diameter and a relatively low SSA [101]. It has been reported that carbonization at high temperatures can produce hydrochars with limited porosity and reduced SSA but with an increased aromatization degree [113]. Therefore, activation is often recommended to improve the porosity and surface area of the hydrochar [54].

(ii) Pyrolysis Technique

Pyrolysis technique is a specialized process that necessitates the use of an inert gas atmosphere to prevent the formation of ash by converting organic matter into a stable, carbon-rich substance by subjecting the biomass to high temperatures and an oxygen-depleted environment. Compared to hydrothermal carbonization, it operates at higher temperatures, resulting in the formation of a unique product known as biochar [26, 101, 114, 115]. After the pretreatment procedure, this technique offers several benefits, including the reduction of water contents and the removal of nutrients and various chemical components such as oxygen, sulphur, hydrogen, and other impurities that may be present in the raw materials. However, it is essential to note that although biochar production effectively eliminated unwanted chemical constituents and impurities, it also reduced the carbon content of materials [116, 117]. That decrease in the carbon content was a result of the thermal decomposition and volatilization of specific organic compounds during the high-temperature process. Despite the possibility of a decrease in the carbon content, biochar retains desirable properties that make it an attractive

material for a variety of applications. The specific properties of biochar can vary based on variables such as the type of biomass used, the operating temperature, the duration of the process, and the inert gas atmosphere used. In general, pyrolysis technique provides a sustainable and ecofriendly method for transforming biomass waste into a valuable, carbon-rich product with a variety of applications and emits syngas, which is not needed for this study [4, 92].

The carbonization or precarbonization technique, also known as the preactivation procedure, will affect the properties of AC materials. This only takes place in the two-step carbonization method for the preparation of AC, which consists of discrete carbonization and activation processes. The techniques used may include pyrolysis and hydrothermal processes. AC carbonized through pyrolysis reveals the highest SSA and total pore volume, with significant micro- and mesopores leading to the highest C_{SP}, energy, and power density when compared to AC carbonized via the hydrothermal technique and a single-step product [60, 73, 74]. Compared to AC produced via the single-step carbonization, AC produced via the two-step carbonization method [75, 76] has a higher SSA with a large number of micropores and a larger total pore volume, resulting in an electrode with greater C_{SP}, lower charge transfer resistance, and superior cycling stability. However, the yield of AC synthesized via two-step carbonization is greater than that from one-step [76]. In addition, it has been reported that an increase in the precarbonization temperature leads to a decrease in SSA and an increase in the volume of micropores and mesopores within AC materials [77]. Precarbonization preserves and modifies the presence of microstructures and heteroatoms in biomass and AC materials [78].

(2) The Effect of Activation Techniques

(i) The Effect of Chemical Activation

In the chemical activation process, a carbon precursor is impregnated with selected chemicals as an activating agent at a preference ratio in a solvent and then heated under an inert environment to enhance the reaction and produce a desired carbon-based product after washing away the impurities and unreacted chemicals. The chemical activation method has been extensively used to produce AC, utilizing activating reagents and low-energy pyrolysis in an inert gas environment to produce the desired carbon-based products [54, 62]. This technique has presented several benefits, including higher AC yields, a large surface area, and a suitable pore size distribution. The selection of an activating agent, which may be a strong base or strong acid, is crucial for enhancing the physicochemical properties of carbon materials, which, therefore, improves their performance [62, 72, 86, 87, 118]. Several activating agents such as potassium hydroxide (KOH) [4, 35, 68, 69, 119, 120], zinc chloride ($ZnCl_2$) [37, 121–124], sulphuric acid (H_2SO_4) [70, 125], nitric acid (HNO_3), sodium hydroxide (NaOH), phosphoric acid (H_3PO_4), and manganese nitrate ($MgNO_3$) have been utilized in the chemical activation process [87]. Each activating reagent influences the activation procedure and the resultant properties of AC differently. It was reported that a single-phase chemical activation technique produced a high yield of AC and influenced the release of volatile compounds [37]. The ratio of the carbon material to activating reagents also influences the pore structure of the AC. A low ratio may result in a reduction in mesopores, while a high ratio may contribute to a reduction in micropores [62]. Thus, the chemical activation method is commonly used and regarded as highly efficient for producing AC with desirable characteristics. By selecting the appropriate activating reagents and controlling process parameters, it is possible to customize pore structures and surface characteristics. Current research in this area aims to further optimize the chemical activation process and investigate novel activating reagents to improve the performance and application potential of AC materials [101].

AC derived from walnut shells was synthesized through chemical activation under different conditions and produced an electrode at a mass ratio of 8 : 1 : 1 AC, carbon black (CB), and PTFE binder, respectively, and nickel foam was used as the current collector. The results showed that the best electrode came from the AC with the highest disorder [59], and they are reported in Tables 1 and 2. AC was produced from banana peels activated with KOH at different temperatures ranging from 750°C to 950°C, wherein the electrode was prepared by mixing 80 wt.% active materials with 10 wt.% carbon black and 10 wt.% polyvinylidene fluoride (PVDF). The as-produced AC at 900°C appeared to be the most effective in 1 M $NaNO_3$. The C_{SP} and energy density increased to 328 F/g and 36.9 Wh/kg, respectively, after being subjected to a voltage holding at 1.8 V for 60 hours at 0.5 A/g [68]. A study was conducted on electrochemical properties of Kanlow switchgrass-derived AC electrodes prepared by direct activation (through a single-step process) and indirect activation (or through a two-step process) with KOH and H_3PO_4. The indirect-process AC was decorated with MnO_2 by the precipitation technique to improve the capacitance performance and cycle life of the electrode, as given in Table 2. However, the direct process AC with KOH performed better [35], as presented in Table 2. As reported in Refs. [26, 35], this could have been caused by the pseudocapacitive behavior in as-

produced ACs due to the presence of a high volume of heteroatoms, which could lead to poor electrochemical performance of the system.

Alternately, other factors were responsible for the poor performance as it has been reported that the enhancement of surface functional groups and control of pore size distribution did not show an improvement in the electrode's performance [36]. AC was produced from olive trees, custard apples, and fig trees through two-phase chemical activation followed by doping with four different oxygen- and nitrogen-rich materials, which are nitric acid (HNO_3), ammonium persulphate ($(NH_4)_2S_2O_8$), melamine ($C_3H_6N_6$), and ammonium carbamate ($H_2NCOONH_4$), to evaluate the effect of surface functional groups on the electrochemical performance of the as-synthesized AC-based electrodes. The doped AC-based electrodes revealed that the higher the oxygen content in the AC, the lower the specific surface area, and the smaller the pore volume, while the higher the nitrogen content, the better the electrochemical performance, with capacitive retention ranging from 97 to 100% [86]. Table 2 lists results for electrochemical properties for the abovementioned and additional studies on AC derived from biomass raw materials.

Chemical activation has been reported to produce AC with higher specific surface area, pore volume, and porosity than physical activation [54, 104] and increase surface functional groups [125]. Akpa and Dagde [104] evaluated the effect of acid (H_2SO_4 and HCl) and base ($ZnCl_2$ and $CaCl_2$) activating agents on the properties of periwinkle shell-derived AC. As the rate of base activating agents increased, pore volume, porosity, and SSA decreased; conversely, as the rate of acid activating agents increased, the reverse occurred. In addition, $ZnCl_2$-based AC has the highest porosity structure, with more micropores and fewer mesopores, as well as an increase in the pore volume, specific surface area, and iodine number. In contrast, activation with H_3PO_4 produces AC with a high concentration of mesopores and macropores [107]. A study was conducted on the activation of carbon xerogel derived from resorcinol-formaldehyde polymeric gel using two different activation techniques, KOH and CO_2 [126]. The KOH activation produces AC with additional micropores that are smaller than 1.2 nm, mesopores with less than 4 nm in size, and defects that are 24 nm in size, which has a significant effect on surface functional groups because it increases oxygen functional groups [126]. Hazelnut shells derived porous carbon prepared by [1] direct pyrolysis of precursors, [2] indirect hydrothermal carbonization followed by pyrolysis of hydrochars, and [3] an indirect mixture of hydrochars with MgO template as an activating agent. The results showed that the porous carbon created with the indirect process [3] (that involves activation) had a lower carbon content of 79.8%, a higher oxygen content of 13.5%, a higher C_{SP} of $323.2 Fg^{-1}$, a higher SSA of $552\ m^2 \cdot g^{-1}$, and a micro-mesoporous interconnection with a higher pore volume of $0.30\ cm^3 \cdot g^{-1}$ that led to a high energy of $11.1\ Whkg^{-1}$ and power density of $156.8 WKg^{-1}$. The product of the indirect method [2] also contained 81.9% carbon, 13.1% oxygen, and a specific surface of $485 m^2 g^{-1}$ with $0.22\ cm^3 g^{-1}$, which is smaller than the product of the method [3, 127].

By synthesizing AC from sago midrid, the effect of chemical activating methods on C_{SP} was evaluated for both $ZnCl_2$ and NaOH, which were used at the same temperature and under nitrogen. $ZnCl_2$ activation resulted in a C_{SP} of $138.36 Fg^{-1}$ followed by NaOH activation resulting in a C_{SP} of $111.37 Fg^{-1}$ [122]. Hierarchical porous carbons derived from corn husk with KOH activating agent at different solution concentrations of 5%, 7%, and 9% carbonized at 800°C. The results indicate that as the KOH concentration increases, the porosity of the produced carbon increases, but the specific surface area, pore volume, and graphitization degree decrease [128]. Leng and Sun [129] synthesized AC derived from coconuts through chemical and physical activation using $ZnCl_2$ activation at 650°C, KOH at 800°C, and water vapor at 800°C. Their resulting ACs reveal a reduction in the mesopore volume with an increase in the micropore volume, total pore volume, SSA from $1250.61 m^2 g^{-1}$ to $3242.05 m^2 g^{-1}$, and C_{SP} from $190 Fg^{-1}$ to $337 Fg^{-1}$ with a capacitive retention of 60% and 98% after 10000 cycles at $1 Ag^{-1}$ as the activation steps were performed. It is evident from these results that the activation process has a significant impact on the physicochemical properties and electrochemical performance of electrode materials. The effect of activating agents on the physicochemical properties of AC synthesized from sago wastes chemically activated with $ZnCl_2$, H_3PO_4 (as acid agents), $KMnO_4$, and KOH (as basic agents) was evaluated. AC from $ZnCl_2$ was found to exhibit the maximum SSA, dominated by well-interconnected pores dominated by the micropore structure with a high concentration of phenol and carboxylate surface functional groups. It was followed by KOH in SSA, which possessed a greater proportion of mesopores with phenol and carbon carboxylate surface functional groups and the highest carbon contents, while ACs produced with $KMnO_4$ and H_3PO_4 activating agents exhibited inferior properties [130]. The analysis of the SEM images and BET results in Figure 2 indicates significant differences in the pore structure of the activated carbons (ACs) prepared using various activating agents as highlighted by the red circles in the images. The AC prepared with $ZnCl_2$ (Figure 2(b)) exhibits a higher abundance of micropores, along with well-developed mesopores

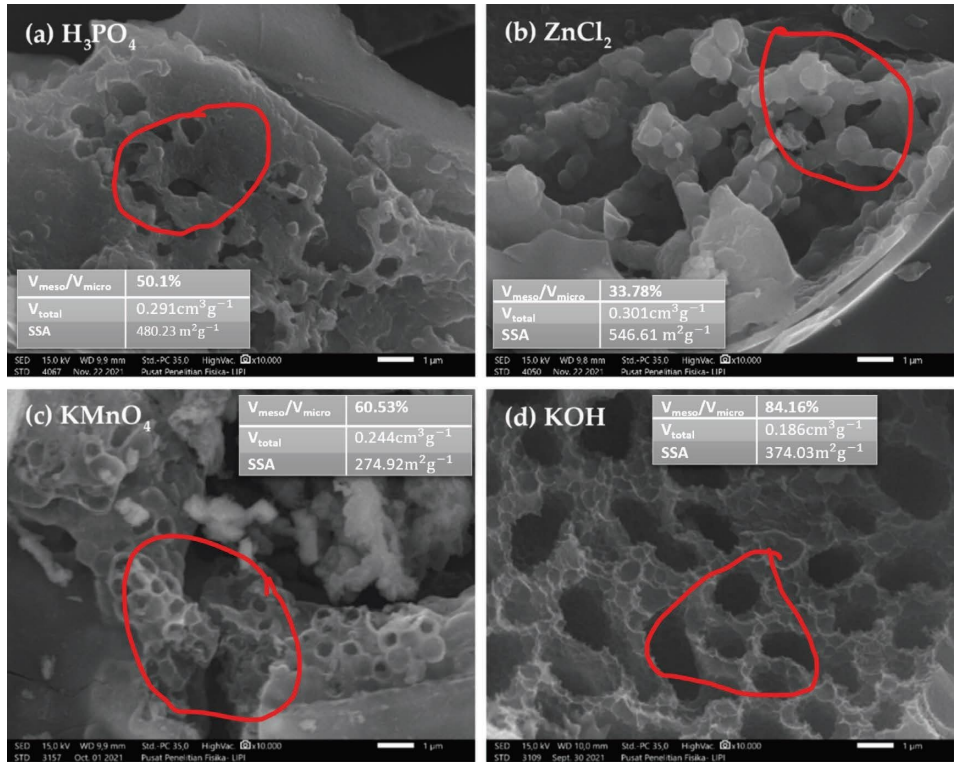

FIGURE 2: SEM images with BET results illustrating the effect of activating agents on the surface morphology of AC derived from sago waste and synthesized by chemical activation. Reprinted from [126] with permission from MDPI.

and interconnected micro-mesopore structures. This results in a larger specific surface area (SSA) compared to ACs activated with other agents (Figure 2(b)). In contrast, the KOH-activated AC (Figure 2(d)) predominantly shows mesopores with minimal micropores. Consequently, it possesses the smallest total pore volume and SSA among the ACs synthesized with $ZnCl_2$, $KMnO_4$, and H_3PO_4 (Figures 2(a), 2(b), and 2(c), respectively). It has been reported that the use of an excessive quantity of KOH leads to a decrease in SSA due to the breakdown of pores [112].

(ii) The Effect of Doping Methods

The doping method is used to introduce specific surface functional groups into carbon materials in an effort to increase their wettability, electrical conductivity, and electroactive surface area, which led to an increase in C_{SP}, charge/discharge rates, and electrochemical stability of the doped carbon materials [131–134]. It has been reported that doping can either be self-doping or introduced doping regarding heteroatoms. Self-doping refers to the occurrence of doping due to the presence of certain chemical constituents such N, P, and S in the carbon precursors, while for introduced doping, dopant precursors were added purposefully to carbon precursors to introduce some of the above-mentioned elements into the carbon structure [135, 136]. As shown in Figure 3, the embedded atoms, or dopant elements, became part of the carbon skeleton structure. Thus, O [137], N [138, 139], P and B [134], and S [135, 139] are frequent doping heteroatoms. Depending on the specific doping element used, these heteroatoms contributed to the formation of different surface functional groups. The choice of the dopant element highly depends on the nature of the material to be doped, and the desired properties based on the intended application. For the purpose of EDLC electrodes, those properties could be charge/discharge rates, C_{SP}, and cycling stability [140, 141].

N-doping increased the electronic conductivity of the doped carbon materials by delocalizing more electrons in the carbon network. Because its atomic radius is identical to that of carbon, it reduces the lattice mismatch in carbon materials. Generally, N-doping increased SSA, improved C_{SP} and cycling stability, and introduced pseudocapacitance behavior that led to high energy density [142–144]. P-doping generated the sp^3 carbon structure with morphological distortion and an open edge that introduced more active sites, which, in turn, caused an increase in C_{SP} [145, 146]. It also increased the voltage window of the storage device, therefore improving electrochemical performance [78, 135]. In addition, increasing the P content enhances the oxidation stability of P-doped porous carbon [147]. B-doping improved conductivity and kinetics of

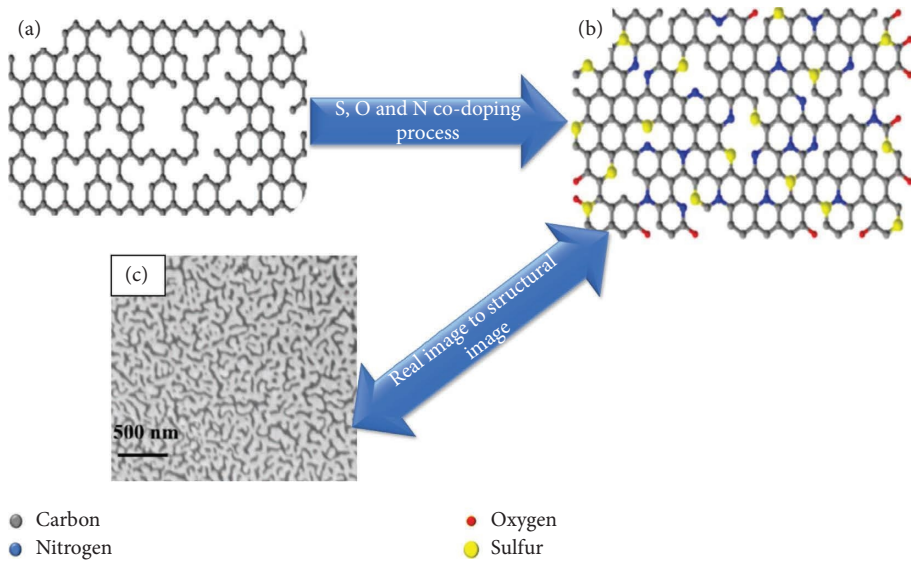

FIGURE 3: Structural images of (a) activated carbon; (b) S, N, and O heteroatoms doped activated carbon; (c) real image from the SEM image of S-, N-, and O heteroatoms doped ginger-derived activated carbon. From a work done by Gopalakrishnan et al. [78] with permission from Elsevier.

charges, which enhanced the cycling stability of doped carbon materials [134, 148, 149], while S-doping created defects in carbon materials that served as active sites for the redox faradaic mechanism by disrupting the carbon structure, thereby enhancing its electrochemical performance [135, 139]. The introduction of faradaic reactions led to pseudocapacitance behavior, which improved the storage capacity, provided excellent cycling stability, and increased the energy density. Therefore, S-doping was more likely to be applied to carbon materials intended to be used in batteries instead of EDLC [78, 150].

The doping method can be implemented via heteroatom codoping or single-element doping. Codoping of heteroatoms entailed the simultaneous introduction of multiple dopant precursors. This technique has demonstrated significant improvements in the C_{SP} of carbon materials, resulting in electrodes with high performance and excellent cycling stability [74, 75]. A variety of dopant precursors have been employed by different researchers; for example, melamine [137] and urea [138] have been utilized as N-dopant sources, CH_4N_2S as N- and S-dopant sources [74], phosphoric acid as the P-dopant source [151], and ammonium borate trihydrate as N- and B-dopant sources [140].

The impact of doping methods on the properties of AC has revealed that heteroatoms influence the modification of surface properties, thereby enhancing the performance of electrodes [147]. The incorporation of heteroatoms into the carbon structure led to the formation of more hydrophilic polar sites, which increased wettability and facilitated the movement of ions from the electrolyte to the active sites of electrodes [152].

To evaluate the impact of operating conditions on the electrochemical performance of carbon materials, B-doped carbon-based electrodes from the coconut shell revealed a decrease in the SSA and the amount of micropore structure of heteroatoms N-, S-, and O-codoped porous carbon as the B-dopant amount increased [153]. Wheat straw-derived carbon was synthesized with salt templating (49% $ZnCl_2$ mixed with 51% KCl) by adding 4 g, 6 g, and 8 g of the same amount of straw and melamine as N-dopant precursors at 0, 0.5, 1, and 1.5 g pyrolyzed at 800°C. The results showed that the carbon material with the highest C_{SP} 223.9Fg^{-1} was obtained from 6 g of added salt, and the effect of the N-doping process was studied using this material. The N content, specific surface area, capacitance, pore volume, and pore size increased as the quantity of melamine increased up to 1 g and decreased as the quantity of melamine increased to 1.5 g, while the C content decreased in the same trend. The carbon from 1 g of melamine has the highest SSA of 1201m^2g^{-1} C_{SP} of 223.9Fg^{-1}, and the pore size was approximately equal to 3.4nm. This carbon was evaluated to determine the impact of silicon (SiO_2) removal. Two methods were applied before and after removal. After 10000 cycles, the postremoval method increased the specific surface area, capacitance, and pore size of the as-produced carbon by 91.4%, while these parameters were reduced for preremoval [137].

Single-step chemical coactivation for the synthesis of B-, N-, and O-codoped laver-derived porous carbon using zinc chloride ($ZnCl_2$) and potassium chloride KCl

activating agents and boric acid (H_3BO_3) as a B-dopant source was conducted. The codoped process is a process of adding two dopants at once on a carbon precursor to introduce impurity atoms in the final product. As-produced laver-derived hierarchical porous carbon materials were designated as B- and N-doped laver-derived hierarchical porous carbon synthesized through $ZnCl_2$ and KCl chemical coactivation (BNPAC-Zn/K), N-doped laver-derived hierarchical porous carbon synthesized through $ZnCl_2$ and KCl chemical coactivation (NPAC-Zn/K), N-doped laver-derived hierarchical porous carbon materials synthesized with $ZnCl_2$ (NPAC-Zn), and N-doped laver-derived hierarchical porous carbon materials activated with KCl (NPAC/K). The as-produced codoped porous carbon exhibited a variety of heteroatoms such as O, N, S, B, and Cl, which introduced pseudocapacitive behavior and increased defects in the carbon skeleton. These demonstrate a 3D microstructure with interconnected hierarchical pores, the largest total pore volume, the highest SSA (see Figures 4(a) (a1 and a2), 4(b) (b1 and b2), 4(c) (c1 and c2), 4(d) (d1 and d2)), high electrical conductivity (see Figure 4(e)), and the highest C_{SP} compared with porous carbon materials produced via chemical activation, as shown in Figures 4(f) and 4(g). In addition, codoped porous carbon has produced supercapacitor cells with enhanced electrochemical performance, whereas 1 mol of sodium sulphate ($1MNaSO_4$) and 1-butyl-3-methylimidazolium tetrafluoroborate/acetonitrile ($1MBMIMBF_4$/AN) have generated an energy density of $29.2Whkg^{-1}$ at a power density of $250Wkg^{-1}$ with a capacitive retention of 92.4% after 10000 cycles at $4Ag^{-1}$ and an energy density of $51.3Whkg^{-1}$ at a power density of $250Wkg^{-1}$ with a capacitive retention of 94.6% after 10000 cycles at $4Ag^{-1}$ [80]. Based on the reported effects and results of heteroatomic doping of biomass-derived carbon materials, N and P dopants have shown the highest and most important impact on the electrochemical performance of the doped carbon-based EDLC electrodes such as enhancing electrical conductivity, increasing surface area that presents more of micropores and mesopores structure, improving wettability, enhancing specific capacitance and stability, and improving thermal stability of electrode materials. Therefore, they can be considered for improving the properties of doped carbon materials and using the optimum amount in order to positively influence electrochemical performance.

(iii) The Effect of Physical Activation Technique

Physical activation can be achieved through a single-phase or two-phase process. For enhanced production of AC, it is recommended to pretreat the raw materials using hydrothermal carbonization or pyrolysis [54]. Consequently, the two-phase process is preferable for this method. In the single-phase process, materials are heated for an extended time at temperatures exceeding those required to produce AC. Physically, AC is influenced by a number of variables, including operating temperature, activating gas, time, and gas flow rate [54, 101, 154]. Activation removes impurities and generates porosity and a large SSA [37]. The activating agent and carbon element in the carbon precursor undergo a reaction at high temperature, leading to the release of carbon and the formation of pores in the carbon structure [54]. The use of carbon dioxide (CO_2) reduces the ratio of micropores to mesopores [62]. This method is relatively simple, safer, and low cost [62, 101]. However, it is time-consuming [101]. The use of CO_2 reduces and converts the quantity, but the process takes too much time unfortunately; compared to chemical activation [62, 105, 155], this method produces AC with a lower SSA and insufficient pore size distribution.

In one study, AC derived from banana peels was produced through a hydrothermal process by adding a powder of banana peels to a solution of deionized water and ethanol and then heating the mixture at 200°C for 24 h. The morphology of the produced AC presented few micropores and macropores and significant mesopores [73]. AC derived from hemp residues was hydrothermally activated through a two-phase process by mixing hemp residues with a 25% H_3PO_4 solution and heating at 200°C for 24 h, and the obtained hydrochar was heated at 450°C for 2 h under N_2 environment. The AC was reheated under N_2 for 15 min at 900°C and then doped with N. Based on the results obtained, the specific surface area, capacitance, and pore volumes decreased as different conditions were applied. This implies that the AC produced at 450°C presented the highest SSA $1630m^2g^{-1}$, C_{SP} $141Fg^{-1}$, and pore volume, among others, whereas the production of the heat-treating process without doping has demonstrated greater electrochemical stability with 86% capacitive retention after 5000 cycles [26]. The impact of activating temperature on the geometrical and porous characteristics of AC derived from high fructose corn syrup and soybean residues was investigated where these materials were hydrothermally carbonized and physically activated at 850°C for 4 h. Soy residues were carbonized through a hydrothermal process followed by physical activation at 850°C [101]. Additional results for biomass-derived AC synthesized through different methods, as shown in Table 1, represent their physicochemical properties, while Table 2 presents their electrochemical properties.

Physical activation has an effect on the properties of AC derived from sago midrid carbonized at 600°C in a nitrogen environment and activated at 700°C in carbon dioxide. The activation with CO_2 led to AC

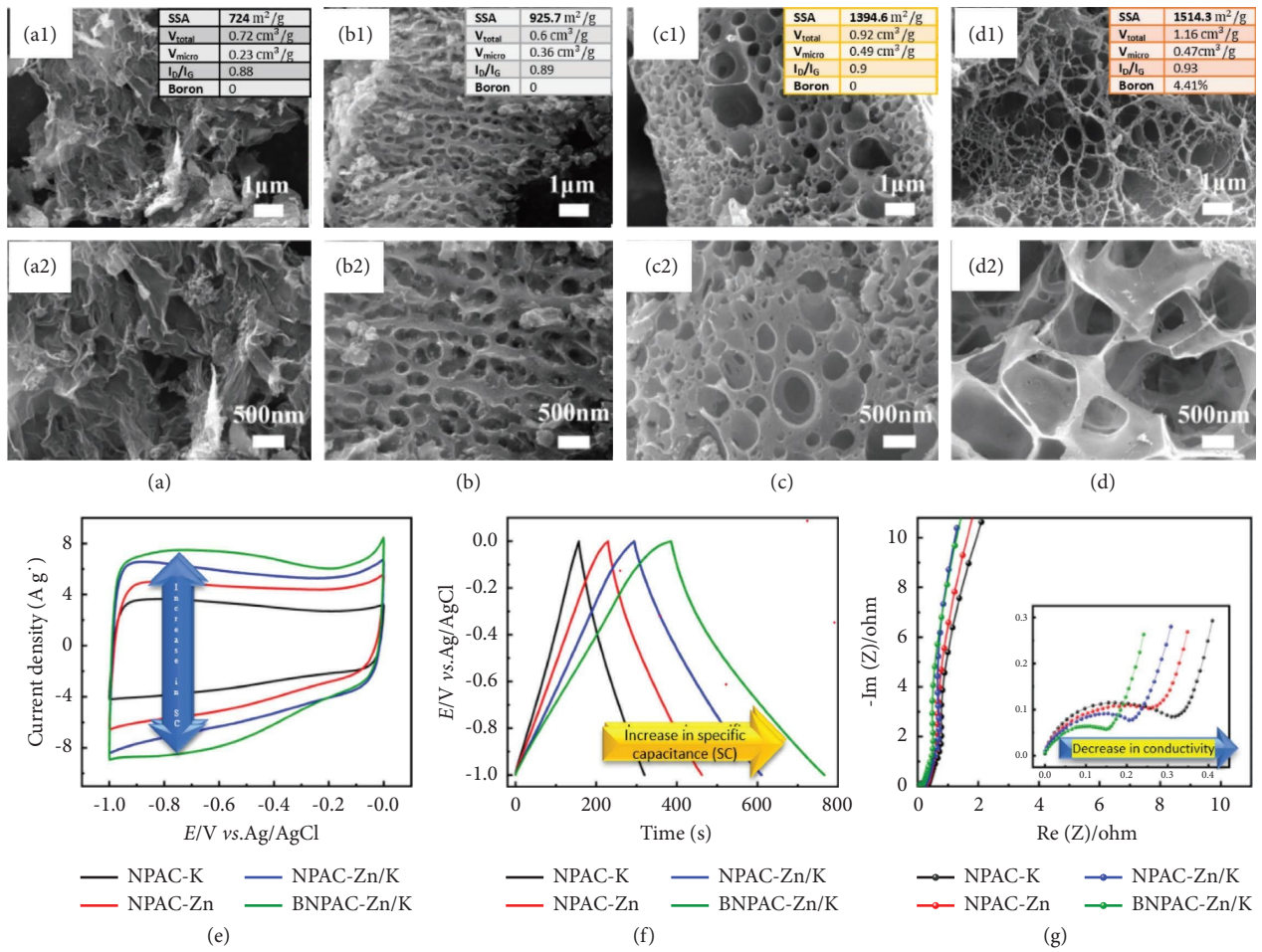

FIGURE 4: Effect of activating agents on physicochemical and electrochemical properties of hierarchical porous carbon materials: (a) (a1 and a2) SEM image of NPAC-K; (b) (b1 and b2) SEM image of NPAC-Zn; (c) (c1 and c2) SEM image of NPAC-Zn/K; (d) (d1 and d2) SEM image of BNPAC-Zn/K; (e) CV curves at 20 mV/s voltage scan rate; (f) GCD curves at 1 A/g current density; (g) the Nyquist figure for all prepared electrode materials from [80], with permission from MDPI.

with a small improvement in micropores and mesopores of less than 10 nm in size, but did not affect the surface functional groups and very small capacitance of 60.8Fg^{-1} [66]. Physical activation with CO_2 at varying temperatures has led to an increase in porosity, SSA [36, 156], and wettability as the temperature increased; therefore, the C_{SP} of the resulting electrode increased. However, the increase in the activating temperature decreased the degree of graphitization of the AC [36]. When the steam rate was increased from 0.5 to 2 cm^3·g^{-1} [105], physical activation in steam showed a small increase in the specific surface area. Activation of AC in steam, CO_2, and air has revealed a reduction in its electrical conductivity. This decrease was due to the formation of additional oxygen functional groups on the surface of the AC. In addition, physically AC has demonstrated a higher electrical conductivity than chemically activated materials [157]. However, physical activation with CO_2 produces AC with a higher SSA and larger pore volume than steam activation [155]. Researchers [158] showed that physical activation under CO_2/steam proportionality led to AC with increasing SSA and pore volume as the amount of steam in the activating environment increased.

(iv) Effect of Templating Method

During the carbonization of raw materials, the template method is commonly used to introduce porosity, and it has been recognized as a promising method for producing AC with a high SSA and controlled pore size distribution [97, 99, 100]. In this process, a carbon precursor and a templating agent are combined, and the resulting mixture is carbonized at a high temperature using the pyrolysis carbonization technique. To remove the template, the as-produced carbon is then washed with a solution tailored to the templating agent [100, 101]. There are two varieties of templates utilized: hard and soft. Hard templates consist of layered silicate, 2D metal hydroxide or oxides, boric acid, 2D transition metal dichalcogenides, molten salts, and ammonium chloride (NH_4Cl) foaming. Soft

templates, on the other hand, are organic molecules with hydrophobic alkyl groups and functional groups capable of forming interaction forces when mixed with appropriate solvents, resulting in the formation of micelles [99, 100]. The micelles interact with the carbon precursor molecules to encapsulate them. Micelles generate apertures during high-temperature carbonization upon decomposition. The subsequent washing or cleansing procedure eliminates the template, leaving the porous carbon material in its place. For soft templates to generate the desired pore structure in the resulting porous carbon materials, they must be able to form nanostructure morphologies and micro- or mesopore components and decompose only after the carbon precursor molecules solidify [102]. Although the soft template method is considered more environmentally friendly than the hard template method, it produces unstable carbon materials. However, the hard template method is highly effective in the production of well-controlled pore size structures, but it requires the complex preparation of hard template agents that do not decompose upon carbon precursor solidification. Therefore, special cleansing procedures of toxic agents that are difficult to remove completly from the as-produced carbon which is a time-consuming processes are required. In addition, the hard template method produces harmful gases and is not environmentally favorable [100]. In general, the template method is an effective technique for customizing the porosity and pore structure of AC materials. The choice between soft and hard templates is determined by the specific requirements of the application, taking into account factors such as porosity control, stability, environmental impact, and synthesis process complexity.

The templating method leads to the production of porous carbon materials with interconnected thin walls and highly disordered microstructure, as presented in Figure 5, resulting in a short diffusion distance for electrolyte ions and increasing the accessibility of active sites within porous carbon electrode materials [159]. This procedure produces porous carbon with a controlled size distribution pores [160]. A study synthesized cotton-derived AC via $ZnCl_2$ activation alone, the magnesium nitrate ($Mg(NO_3)_2$) template method alone, and a combination of $Mg(NO_3)_2$ template with $ZnCl_2$ activation in a single step. The combination produced AC with the lowest graphitic structure, the highest intensity ratio, the largest SSA with abundant and clear porosity, and the lowest equivalence series resistance when compared to other methods. The template method was employed to produce AC, and the activated sample exhibited the lowest intensity ratio, indicating the highest graphitization degree, which slows the transmission of ions [72]. Sodium carbonate (Na_2CO_3) has been used as a salt template in the synthesis of gluconic acid-derived porous carbon using freeze-drying and pyrolysis at a high temperature. The use of Na_2CO_3 led to an increase in the oxygen content of porous carbon materials and presented pseudocapacitive behavior, which enhanced the electrochemical performance of Na-ion capacitors [159]. In one study, the use of sodium phytate at different mass ratios (0, 1, 2, and 3) revealed an increase in the specific surface area, pore volume, and diameter with the amount of meso- and macropores and C_{SP} as the ratio increased, but the best performance was observed in porous carbon materials with a mass ratio of 2 [82]. The use of cobalt nitrate ($Co(NO_3)_2$) as a template in the synthesis of porous carbon materials has led to the formation of interconnected cavities with thin walls, which decreases the charge transfer resistance of the as-produced porous carbon. It has also increased the formation of graphitic structures with a small degree of disorder within the carbon, which enhances its electrical conductivity and, therefore, improves its electrochemical performance [161].

2.2.2. Effects of Carbonization/Activation Time. Carbonization and activation time have an impact on the properties of the as-produced carbon [101, 162]. Studies on the synthesis of AC from walnut shells (WSs) at 900°C for different activation times (75, 90, and 105 minutes) revealed that the activation time affected the pore size in the derived AC. As the activation time increased, the quantity of micro- and mesopores increased. The walnut shell-derived AC for 105 minutes (WS-105) showed the lowest intensity ratio of D to G bands, and the extended activation time produced AC with a higher degree of graphitization, as shown in Figure 6(d). In addition, the walnut shell-derived AC produced for 90 minutes (WS-90) exhibited the highest SSA and pore volume that led to the best overall electrochemical performance [59], as shown in Figure 6. In addition, a long time period of carbonization has led to a high resistance material as shown in Figure 6(c). Increasing the activation time from 1 h to 3 h led to an increase in the total SSA and micropores portion [101]. Increasing the activation time decreases the pore size and volume of mesopores [101, 155]. A study conducted on AC derived from sargassum for different activation times has not shown a clear correlation with AC morphology, but some effects were observed in the SSA, pore volume, and materials stability [163]. The SSA and pore volume increased with increasing activation time [162]. Referring to Figure 6, the activation time highly affects the physicochemical and electrochemical properties of biomass-derived porous carbon materials.

2.2.3. The Impact of Mass Ratio of Activating Agent to Biomass Raw Materials. This ratio is also known as the impregnation ratio. The impregnation ratio has a substantial effect on the morphology (the total pore volume, average pore diameter, and specific surface area) [153, 163, 164],

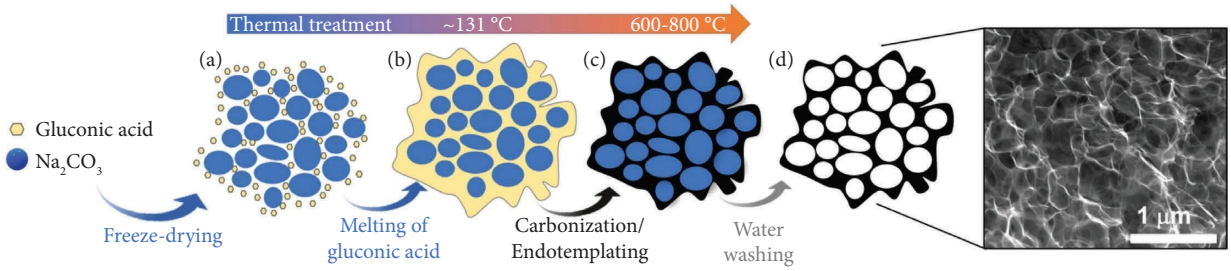

FIGURE 5: Schematic diagram of the salt templating as a hard-templating agent approach used for the production of porous carbon materials: (a) freeze-drying of templating agent and carbon precursor mixture; (b) the melting of the mixture; (c) the carbonization of the mixture; (d) the washing of carbonized carbon. Figures were sourced from [159] with permission from Wiley.

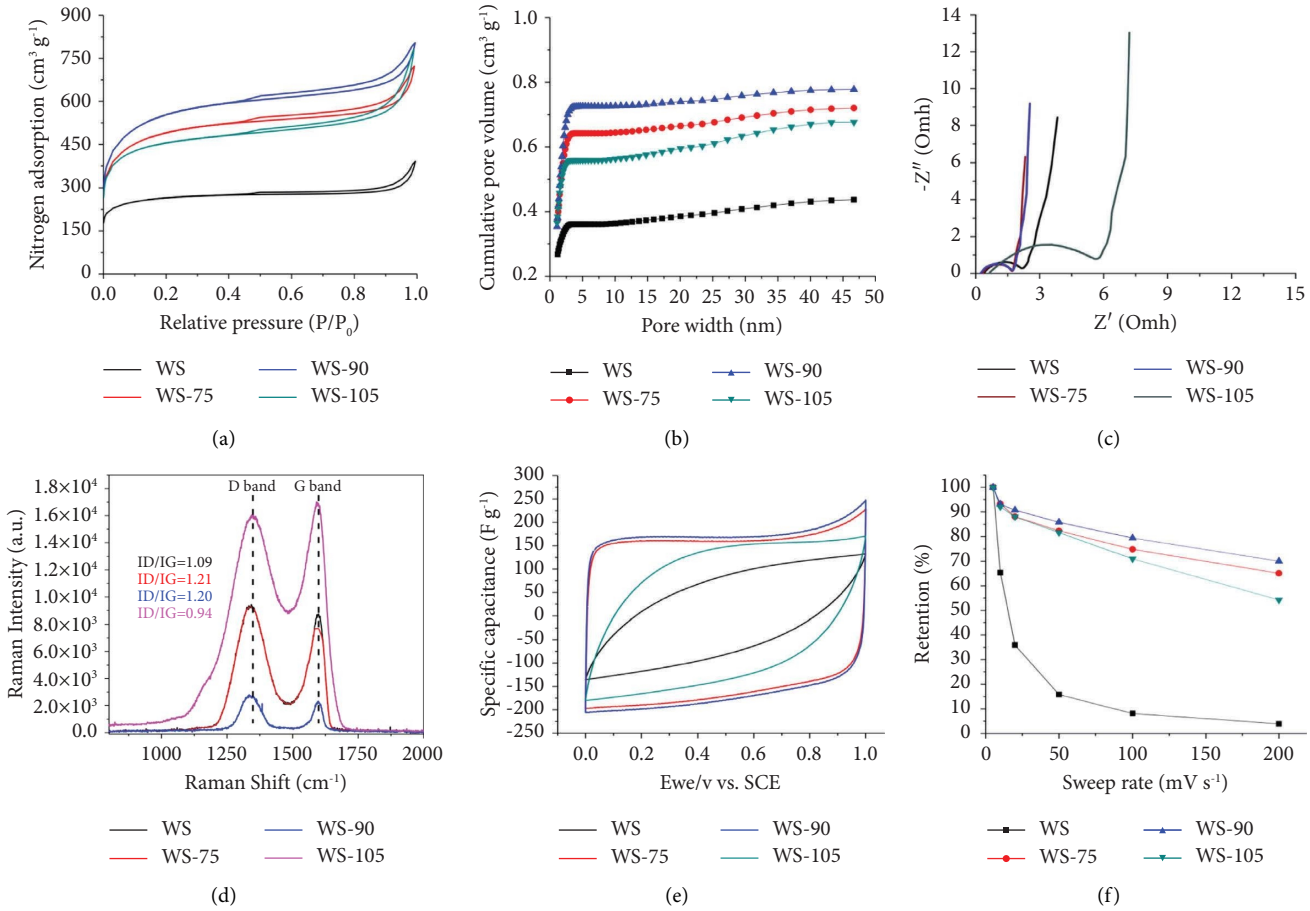

FIGURE 6: Effect of activation time of the walnut shell synthesized for 0 (WS); 75 (WS-75); 90 (WS-90); 105 (WS-105) minutes: (a) N_2 isothermal adsorption/desorption; (b) cumulative pore volumes; (c) Nyquist plots; (d) Raman spectra curves; (e) cyclic voltammograms curves; (f) capacitive retention ratio as a function of potential sweep rate. Figures were collected from [59] with permission from Elsevier.

surface functional groups, and electrochemical performance [85, 164, 165] of the AC. As the mass ratio of biomass materials to activating agents decreases, the SSA increases [153, 164]. In producing AC from tree bark with (KOH) as the activating agent, various mass ratios of 1 : 1, 2 : 1, and 3 : 1 did not affect the AC in terms of mass ratio difference [65]. In a study on resorcinol-formaldehyde polymeric gel derived from activated KOH, the 6 : 1 ratio of KOH to carbon performed better with a long discharging time, indicating a high capacitance of 222Fg^{-1} at 0.1Ag^{-1} with 97% retention capacity after 1000 cycles and ESR of 0.77 Ω [66]. AC derived from the desiccated coconut residue was prepared by impregnating biochar with sodium hydroxide (NaOH) at 1 : 1, 2 : 1, and 3 : 1 ratios (NaOH to biochar) at 500°C and 800°C, revealing an increase in the SSA, micropore, and mesopore volume as the ratios increased. In addition, impregnation of a 3 : 1 ratio at 500°C produced AC with the highest SSA, highest micropore, and mesopore, as well as total pore volumes [166]. The synthesis of bell pepper seeds impregnated at different ratios of potassium bicarbonate ($KHCO_3$)

to the mass of precursor and carbonized at 850°C revealed that the best ACs were obtained at 1 : 1. This material exhibited a high electrochemical performance stability with 99% coulombic efficiency after 25000 cycles [167]. The synthesis of AC from green tea carbonized at 800°C and with KOH at different weight ratios of 1, 3, and 5 of KOH to green tea at 800°C revealed an increase in the SSA, pore volume and diameter, C_{SP}, and cycling stability as the ratio increases. In addition, the as-produced AC-based electrode displayed energy and power densities of 142Whkg^{-1} and 3192Wkg^{-1}, respectively [85]. In AC, a very low ratio prevents the formation of pores, while a very high ratio leads to the collapse of pores within the AC [168].

The mass ratio of the activating agent to AC affects the properties of as-produced ACs. Researchers [169] synthesized AC from willow wood via chemical activation with KOH at KOH/C mass ratio (0, 1, 3, 6, and 9). As the ratio increases, the degree of disorder, SSA, total pore volume, and micro- and mesopore volumes of the AC increase, leading to an increase in electrodes with increasing C_{SP}, capacitive retention, and electrical conductivity. Increasing the ratio of the activating agent to carbon mass ratio from 0 to 4 led to an increase in the SSA and pore volume, which decreased when the ratio exceeds 4. This indicates that excess activating agents occupied active sites within carbon [162]. Synthesis of cashew nutshells with KOH activation revealed an increase in pore size as the ratio of activating agent to carbon precursor increased from 1 to 2, but decreased for other ratios [170], while the synthesis of AC from coffee grounds with KOH at 1 to 10 mass ratios revealed an increase in the SSA, total pore volume, mesopore volume, and C_{SP} as the ratio was increased up to 8, and a decrease was observed when the ratio reached 10. This indicates that the optimum ratio of the activating agent to the carbon material was 8 [171]. Table 3 disclosed that the mass ratio influenced the surface morphology of AC and thus their electrochemical performance, as shown in Figure 7. From the abovementioned results, the impregnation ratio is one of the factors that influence the physicochemical and electrochemical properties of biomass-derived AC. The saturation point varies from one material to another. Therefore, it has to be carefully adjusted and optimized for the production of high-quality AC electrode materials from biomass to generate a high-performance EDLC.

2.2.4. Effects of Operating Temperature. Operating temperature affects the morphology and texture of AC [63, 173], as shown in Table 3, and has a substantial effect on the electrochemical performance of electrode materials [66, 163, 174], as reported in Figure 7. Preactivation temperatures influence the morphology and performance of electrode materials [175]. EDLC exhibits excellent electrochemical performance properties at 850°C [4]. The temperature increase from 750°C to 900°C has led to an increased SSA and micropore volume [68]. By increasing the temperature beyond 750°C, micropores and mesopores were produced [68]. The volume of micropores decreased as the temperature was above 500°C, while the volume of mesopores increased [37]. In one study, an increase in the temperature from 700°C to 800°C enhanced the capacitive performance of the AC by increasing the SSA and micropore volume [58]. The increase in the temperature led to increases in SSA and pore size [71]. The increase in the temperature from 500°C to 900°C led to an increase in the volume and SSA of micropores, while there was a decrease at 800°C and no significant change in dimensions of the mesopores. Furthermore, an increase in the carbon content was observed as well as a decrease in oxygen or surface oxygen functional groups and hydrogen contents as the operating temperature increased. As the operating temperature increased, a significant crystalline structure was observed in the produced ACs, which influenced the electrical conductivity. The electrical conductivity was low, and it started to increase as the temperature increased from 500°C to 700°C and then reduced and remained constant from 700°C to 800°C and 800°C to 900°C. The Coulombic efficiency value indicates the stability of the material with the highest value indicating excellent reversibility across a range of current [66]. However, low temperatures produce carbonaceous materials with poor electrical conductivity [4]. By increasing the activation temperature from 900°C to 950°C, the produced AC degree of disorder and SSA decreased. Similarly, by increasing the temperature from 750°C to 900°C, the degree of graphitization decreased [68], and increasing the temperature from 800°C to 1000°C decreases the SSA, the oxygen content, and the capacitance performance [58]. The increase in the temperature from 600°C to 800°C decreases the nitrogen and oxygen [71]. This shows that temperature influences the properties of biomass-derived carbon-based electrodes.

In one study, AC derived from the bark of Acacia auriculiformis and produced at three different temperatures 600°C, 700°C, and 800°C revealed that as temperature was increasing, the SSA and the pore volume increased, with a high concentration of micropores, leading to the highest SSA. The AC produced exhibited the highest current at 700°C, resulting in the highest capacitance of 191Fg^{-1}. Therefore, this temperature was selected as the optimum activation temperature for this material. In addition, researchers observed that the high temperature destroys suitable porous structures, therefore limiting ion transportation and charge storage capacity of the AC produced at 800°C [65]. AC derived from the desiccated coconut residue was prepared in two steps and at three different temperatures. The results revealed that at the same impregnation ratio, the carbon content and microporous increased, but the oxygen content reduces as the temperature increased [166]. A study was conducted on hazelnut shells carbonized hydrothermally at different temperatures (175°C, 200°C, and 220°C) and different carbonization times (4, 6, 8, 10, and 12 h). The hydrochar produced at 200°C for 8 h had the highest SSA of 552m^{2}g^{-1} and pore volume of 0.30cm^{3}g^{-1}. They have also observed that as the temperature of carbonization increases, the oxygen content of carbon reduces [127]. In one study, the effect of activation temperature on the morphology, SSA, and degree of graphitization of puffed-rice AC was synthesized in two

Table 3: The effect of the mass ratio of the activating agent to the (CMS) carbon molecular sieve (at 0.5, 1, 2, 3, and 4 ratios) combined with activating temperature (700, 800, and 900°C) on the surface morphology and texture of activated carbon molecular sieve (AMS).

Sample	N_2 sorption				Total pore volume[e] ($cm^3 \cdot g^{-1}$)	Average pore size[f] (nm)
	S_{BET}[a] ($m^2 \cdot g^{-1}$)	S_{micro}[b] ($m^2 \cdot g^{-1}$)	S_{meso}[c] ($m^2 \cdot g^{-1}$)	Ratio[d]		
AMS–0.5–700	110	104	6	17.3	0.07	0.54
AMS1–700	334	308	26	14.1	0.18	0.53
AMS2–700	375	348	27	15.7	0.21	0.53
AMS3–700	403	362	41	8.8	0.22	0.55
AMS4–700	507	442	65	6.8	0.25	0.55
AMS0.5–800	464	425	39	10.9	0.23	0.58
AMS1–800	660	602	58	10.3	0.32	0.68
AMS2–800	695	629	66	9.5	0.37	0.68
AMS3–800	797	693	84	8.3	0.33	0.65
AMS4–800	958	852	106	8	0.4	0.63
AMS0.5–900	757	654	103	6.4	0.43	0.63
AMS1–900	872	745	127	5.9	0.50	0.66
AMS2–900	904	756	148	6	0.56	0.73
AMS3–900	918	744	174	4.3	0.57	0.67
AMS4–900	1410	841	569	1.5	0.8	0.7

[a]BET surface area. [b]Microporous surface area calculated by the t-plot method. [c]Mesoporous surface area. [d]Micropore/mesopore surface area ratio. [e]Total pore volume. [f]Average pore size. Copied from [172] with permission from Elsevier.

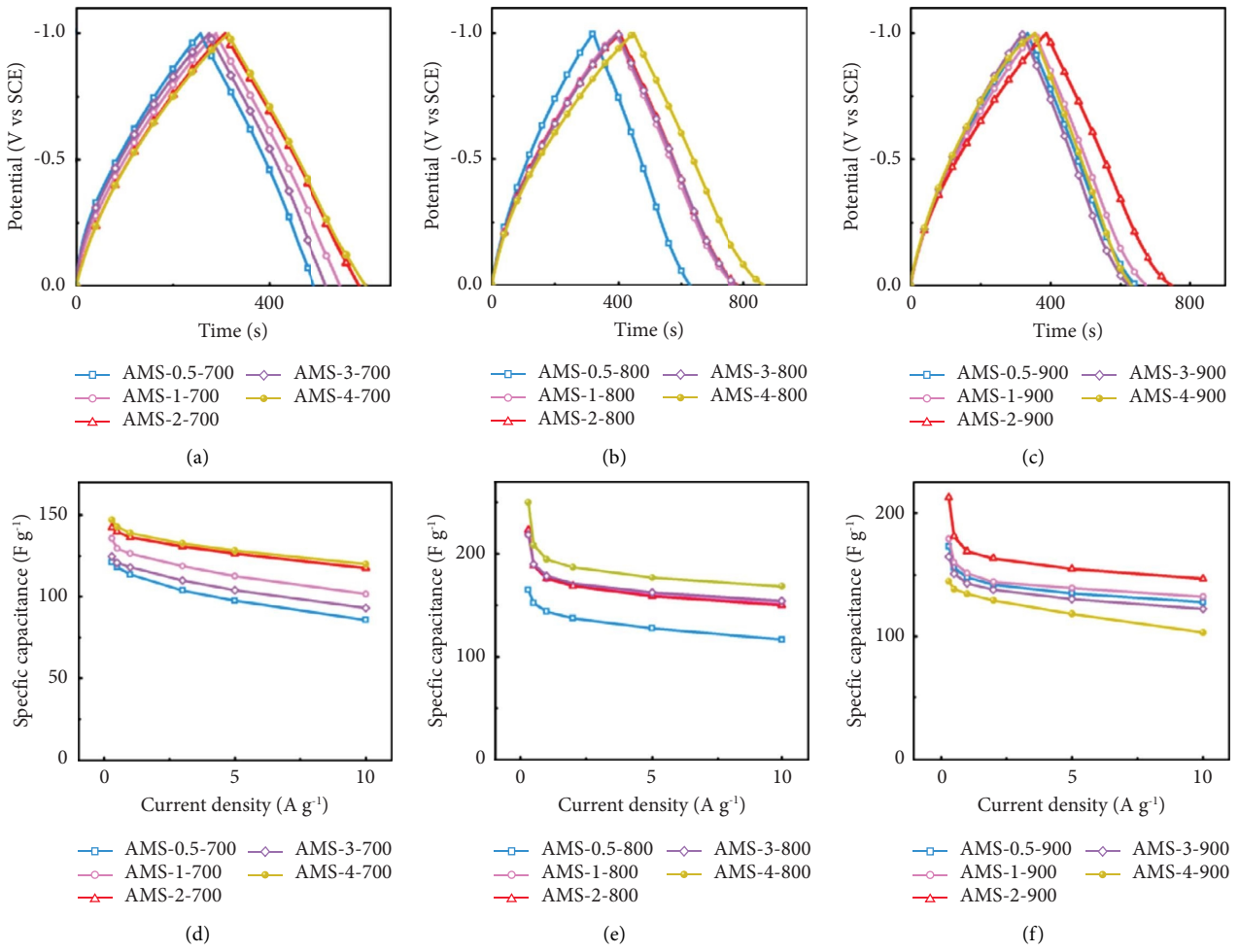

Figure 7: Electrochemical performance of AMS-*x*-*y* based electrodes (*x* represents the mass ratio, and *y* represents the activation temperature) tested: GCD curves at 0.5 $A \cdot g^{-1}$ of (a) AMS-*x*-700, (b) AMS-*x*-800, (c) AMS-*x*-900; specific capacitances at different current densities of (d) AMS-*x*-700, (e) AMS-*x*-800, and (f) AMS-*x*-900. Copied from [173] with Elsevier permission.

steps, and they were carbonized at 500°C and activated at 750, 800, 850, and 900°C. Compared to other temperatures, the AC produced at 800°C had the highest intensity ratio (I_D/I_G) of peaks D to G, which indicates the lowest degree of graphitization and the highest defect degree with disordered carbon atoms. Its morphology has shown an increase in the sheet-like structure with exposed bulges. Additionally, the AC with the best SSA of 1635.0m^2g^{-1} displayed C_{SP} of 117.2Fg^{-1} and ESR of 0.31 Ω [176]. The corncobs were chemically activated through a two-phase process in which carbonization was conducted at 400°C with a flow rate of 3°C min^{-1} for 4 h. The produced carbon was impregnated with KOH and activated at 800°C to 900°C with different flow rates from 3°C min^{-1} to 10°C min^{-1} for 1 to 3 h. The electrode was prepared by mixing 80 wt.% AC with 15 wt.% CB and 5 wt.% PTFE. Their morphological analysis has revealed that 49% of the pore size distribution of the carbon activated at 850°C consisted of micropores. Among the three distinct activation temperatures (650°C, 750°C and 850°C), the AC that was produced at 850°C has shown the highest performance [4].

The effect of activation temperature on the capacitive performance of AC derived from karagash and pine sawdust was evaluated. The synthesis of both precursors involved hydrothermal carbonization followed by chemical activation at different temperatures. A temperature increase led to an increase in graphitization degree and a decrease in C_{SP} for both precursors [64]. In one study, an increase in the temperature revealed a reduction in the density and the diameter of nanofibers formed on the surface of AC. However, the porosity, SSA, carbon content, and the capacitive and physicochemical properties of AC were enhanced [177]. The SSA and pore volume increased with activation temperature to the optimum value of 800°C but decreased when the activation temperature was increased above the optimum value [162]. In another study, activation of Prosopis juliflora wood from 700°C to 900°C revealed an increase in the O content, C content degree of disorder, SSA, pore volume, and C_{SP} with a reduction in charge transfer resistance and ESR. Hence, the as-produced porous carbon-based electrode materials performed well [178]. The increase in the activation temperature has led to a decrease in the charge transfer resistance, leading to an upsurge in the electrical conductivity of porous carbon materials [179]. The increase in the carbonization temperature revealed an increase in the SSA, micropore volume, and total pore volume but a decrease in C_{SP} when the temperature exceeded that of the porous carbon prepared from Perilla frutescens [180]. This indicates that the optimum carbonization temperature for this material is 700°C. In addition, it has been reported that the heating rate significantly affects the textural and morphological properties of AC [63].

Briefly, higher operating temperatures increase the porosity, SSA, and graphitic degree and influence the mechanical stability by increasing the C content, which leads to a rise in the storage capacity and electrical conductivity, which upgrades charge/discharge rates, reduces crystallinity, and preserves or removes some surface functional groups that influence the electrochemical performance of EDLC electrodes. Unambiguously, regarding the synthesis of biomass-derived porous carbon materials, there was no universally applicable optimal carbonization/activation temperature for the synthesis of all biomass-derived porous carbon reported. This was a result of the inherent differences in physical and chemical properties between various biomass materials.

2.3. Physicochemical Properties of Porous Carbon Materials. The physicochemical properties of active materials are known to determine the electrochemical efficiency of the EDLC electrode [54, 69, 101]. This section describes the effect of some physicochemical properties on the electrochemical properties and performance of electrodes in EDLC. These properties include the surface functional groups, specific surface area, pore structure and distribution, crystallinity, and thermal conductivity of biomass-derived AC.

2.3.1. Effects of Surface Functional Groups. Surface functional groups are also identified as factors influencing the electrochemical performance of electrode materials [23, 24, 26, 181]. However, surface functional groups can increase the reactivity of electrode materials with electrolyte, which can lead to carbon degradation [182]. It has been reported that the presence of carboxylic groups improves the wettability of the surface and decreases the resistance of ACs, thereby enhancing the electrochemical performance of electrode materials [67, 164]. The presence of heteroatoms enhances the surface wettability and electronic conductivity of AC, resulting in an electrode with enhanced electrochemical performance [4, 86]. Heteroatoms enhance materials' capacitance, energy, and power densities [86]. Functionalities on the surface provide a stabilizing effect [182]. The presence of the nitrogen group improves the electrochemical stability, wettability, and conductivity of AC [69, 181, 183, 184]. The presence of a nitrogen group reduces the ash content of AC [26]. It also enhances the energy density of the fabricated electrical double-layer capacitors without sacrificing their cycling stability [143].

The oxygen content and its different functionalities have different impacts on the electrode conductivity, wettability, and faradaic behavior [142, 164]. A high concentration of oxygen functional groups enhances the ion transfer and decreases the mass transfer resistance [35]. Combining a higher oxygen content with sufficient mesopores increases the electrolyte accessibility, fast ion transport, and higher capacitance [86]. Unfortunately, the presence of very high oxygen functional groups leads to pseudocapacitive behavior in AC, which reduces the electrochemical performance of the system [26, 35, 86, 180]. The very low oxygen content has led to poor performance, despite the presence of high micro-mesopore interconnection [185].

Therefore, the optimum oxygen content and functional groups are required to increase the electrical conductivity and electrochemical stability of materials without compromising their performance [26]. The presence of surface quinone increases the capacitance of oxidized AC through

pseudocapacitance by increasing the ohmic resistance [77, 86]. The presence of C-O and C=O at the edge of the basal planar or on the outer surface produces an acidic physical appearance that facilitates rapid ion transport and increases the hydrophilicity of the electrode [66], while the presence of resonating electrons in the aromatic ring, also known as the basicity of oxygen functionalities, is responsible for faradic behavior [142]. The increase in conductivity improves the characteristics of micropores [185]. The increased wettability of the internal structure of electrode materials due to the presence of polar oxygen groups increases the interaction between the electrode and electrolyte, resulting in a higher C_{SP} of electrode materials [127].

The impact of oxide functional surface groups such as magnesium oxide (MgO), phosphorus pentoxide (P_2O_5), sulphur trioxide (SO_3), potassium oxide (K_2O), calcium oxide (CaO), manganese oxide (Mn_3O_4), and iron(III) oxide (Fe_2O_3) on the electrochemical performance of AC was evaluated. The presence of oxide functionals led to the formation of stratified and perforated AC, which improved the C_{SP} and cycling stability of AC materials by introducing pseudocapacitive behavior in the as-produced ACs [89]. It was observed that AC with an average O_2 and high N and S quantity with a good carbon content exhibited the highest SSA and total pore volume, as well as the lowest charge transfer resistance and ESR, resulting in the highest C_{SP} and good energy density [74]. The N-doping of porous carbon materials enhances the electron and ion transfer kinetics at the electrode/electrolyte interface. The presence of N/O functional groups in a porous carbon skeleton increases electrolyte infiltration into the active materials of an electrode [186]. As shown in Figure 8(c), related to Figures 8(d), 8(e), and 8(f), the surface chemistry highly influenced electrochemical performance.

2.3.2. Effects of Surface Morphology. The surface morphology of a porous carbon material refers to a combination of its SSA, pore structure, distribution, and pore size. The pore distribution affected the electrochemical properties of electrodes [7, 61]. A fine pore distribution has improved the kinetics of electrodes [60, 187]. Due to the charging/discharging mechanism of EDLC known as the electrostatic double layer, which took place at the electrode/electrolyte interface, electrodes' SSA played a very vital role that influenced their electrochemical performance. The larger SSA of electrodes facilitated the faster adsorption/desorption of electrolyte ions into electrodes, meaning that greater charges were stored, which resulted in an increase in the C_{SP}, high energy density, and power density. In addition, by providing enough active sites in a larger SSA, the internal resistance is reduced and the cyclic stability is enhanced [46, 188–191]. As the pore volume determines the interaction between the electrode's surface and electrolyte, a larger pore volume facilitates the kinetic and diffusion of electrolyte ions, which leads to an increase in the storage capacity, excellent rate capability, and high power density of electrodes [192–194]. Pore volume was defined as the total volume of micropores, mesopores, and macropores present in the carbon. It has been reported that the appropriate pore size distribution enhanced the accessibility of electrolyte ions, thereby contributing to the electrode's storage capacity, which led to high energy and power outputs [195]. The micropore area influenced the active SSA, which contributes towards higher C_{SP}. The larger the micropore area, the wider the SSA is available to store more charges, which increases the storage capacity by enhancing the interaction and confinement of electrolyte ions and leads to an enhanced rate capability and cyclic stability. Therefore, the micropore area influences the electrochemical performance of electrodes [60, 139, 196–198]. Mesopores facilitate the movement of ions and lead to a supercapacitive behavior and high power output, thereby improving the electrochemical performance of the electrode [139, 187, 197], while macropores facilitate the penetration of electrolyte ions [61, 187, 197] by acting as a reservoir for electrolyte ions [112]; they also reduce the distance between the active sites and ions [199]. In addition, the size of solvent molecules and solvated ions must be larger than the pore diameter for the ions to migrate easily through the micropores [7, 68, 187, 196].

A study was conducted on AC derived from wheat husks, and their results revealed a correlation between pore size distribution and the electrochemical performance of the system. The SSA of the AC with a higher micropore volume than the mesopore volume is smaller, while AC with a smaller micropore volume than the mesopore volume exhibited the highest SSA and presented the best electrochemical performance. However, a porous carbon with an adequate quantity of mesopores and sufficient micropores distribution structure demonstrated high electrochemical performance and excellent cycling stability with 98.5% capacitive retention after 30000 cycles at $5Ag^{-1}$ [198]. AC with a greater quantity of micropores compared to mesopores, but with sufficient mesopores, produces an electrode with high electrochemical performance and excellent cycling stability with high capacitance retention [164, 175, 200]. The presence of abundant pores on an electrode's surface area facilitates the transport and adsorption of electrolyte ions and the accumulation of charges [72].

Because ions can easily diffuse from pores/channels to others, a structure of interconnected and distributed micromesopores reduces the ion transport resistance and prevents ion deposition. A poor pore connection leads to insufficient ion diffusion, high ion transport resistance, impasse, and misrepresentation of pores. Hence, more ions are deposited in pores and channels, resulting in decreased cycling stability and capacitance retention [129, 201]. The results of the study conducted on sargassum-derived porous carbon (SPC-*x*, where *x* represents the activating agent to carbon precursor mass ratios, which are 1, 2, and 3) for SPC-1, SPC-2, and SPC-3 revealed SSA with $1500.5m^2g^{-1}$, $2019.9m^2g^{-1}$, and $2103.2m^2g^{-1}$ with $1.1cm^3g^{-1}$, $1.2cm^3g^{-1}$, and $1.5cm^3g^{-1}$ total volumes, achieving a C_{SP} value of $301Fg^{-1}$, $194.5Fg^{-1}$, and $209Fg^{-1}$, respectively. Figure 9 shows that SPC-1 had a larger quantity of micropores and an average of mesopores, which contributed to its high C_{SP} [179]. These results indicate that it was not only higher SSA and total pore volume that led to a higher C_{SP} and electrochemical

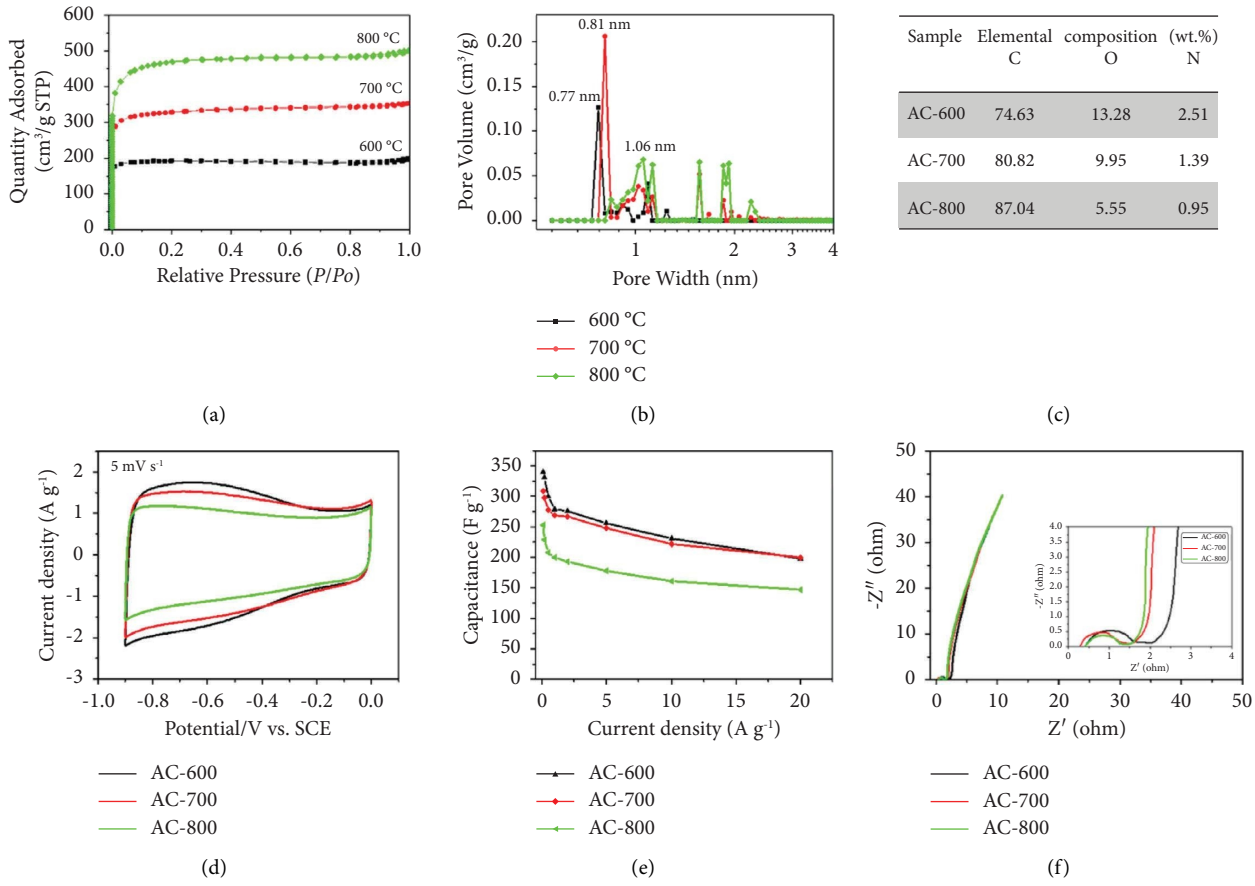

Sample	Elemental composition (wt.%) C	O	N
AC-600	74.63	13.28	2.51
AC-700	80.82	9.95	1.39
AC-800	87.04	5.55	0.95

FIGURE 8: Consequence of the surface structure and surface chemistry of willow catkins-derived activated carbon (activated at 600, 700, and 800°C temperatures) on the electrochemical performance of the based electrodes: (a) nitrogen adsorption desorption isotherm; (b) pore size distribution curves; (c) a table of chemical composition; (d) cyclic voltammetry curves; (e) dependence of specific capacitance and current density; (f) the Nyquist plot. All figures were copied from [104] with permission from Elsevier.

performance but also the pore structure and distribution as additional factors that led to electrodes with high electrochemical performance.

A high ratio of micropore volume to the total pore volume leads to a high SSA, high electrical conductivity, C_{SP} with high capacitance retention, high energy density, high power density, and lower ESR [202]. The C_{SP} decreased as the volume ratio of micropores to mesopores decreased [203]. In addition, it is crucial to understand that the average pore size must be proportional to the size of electrolyte ions for easy penetration into the active sites of porous carbon materials, as was revealed for porous carbon materials with the largest average pore size, which exhibited excellent electrochemical performance and cyclic stability [172]. Therefore, a well-interconnected micro-mesopore structure with an adequate quantity of micropores and mesopores is required to increase the accessibility of active sites in electrode materials, leading to rapid ion motion and minimizing the diffusion distance, which results in the long cycling stability and improves the storage capacity of the device. As shown in Table 4, carbon materials with a larger SSA are not the only key to achieve excellent performance in EDLC as they must be associated with well distributed and interconnected pores with a variety of surface functional groups or heteroatomic surface chemistries, as shown in Figure 8. The micropore/mesopore volume ratio greater than one increases the total volume, and SSA influences the electrochemical properties of porous carbon materials, but they are not the only factors that determine the performance of electrodes or devices based on porous carbons.

2.4. Effects of Mass of Active Materials and Thickness of Electrode. High-loaded mass leads to a high capacitance of the electrode; therefore, more energy is stored [21, 214]. The outputs of an EDLC power and energy density are determined by the mass of active materials [21]. However, it has been observed that the capacitance of the electrode decreases as the mass of the AC material increases [215]. Therefore, optimizing the mass is one of the essential requirements to produce a high-performance electrode. The thickness of the electrode determines the power and energy density of the EDLC system. It has been reported that an electrode with a thickness of several tens of micrometers generates a high power density, while an electrode with a thickness of several hundreds of micrometers produces a high energy density device [216]. A thin electrode can lead to an incorrect estimation of its electrochemical performance [217]. Many commercial electrodes in

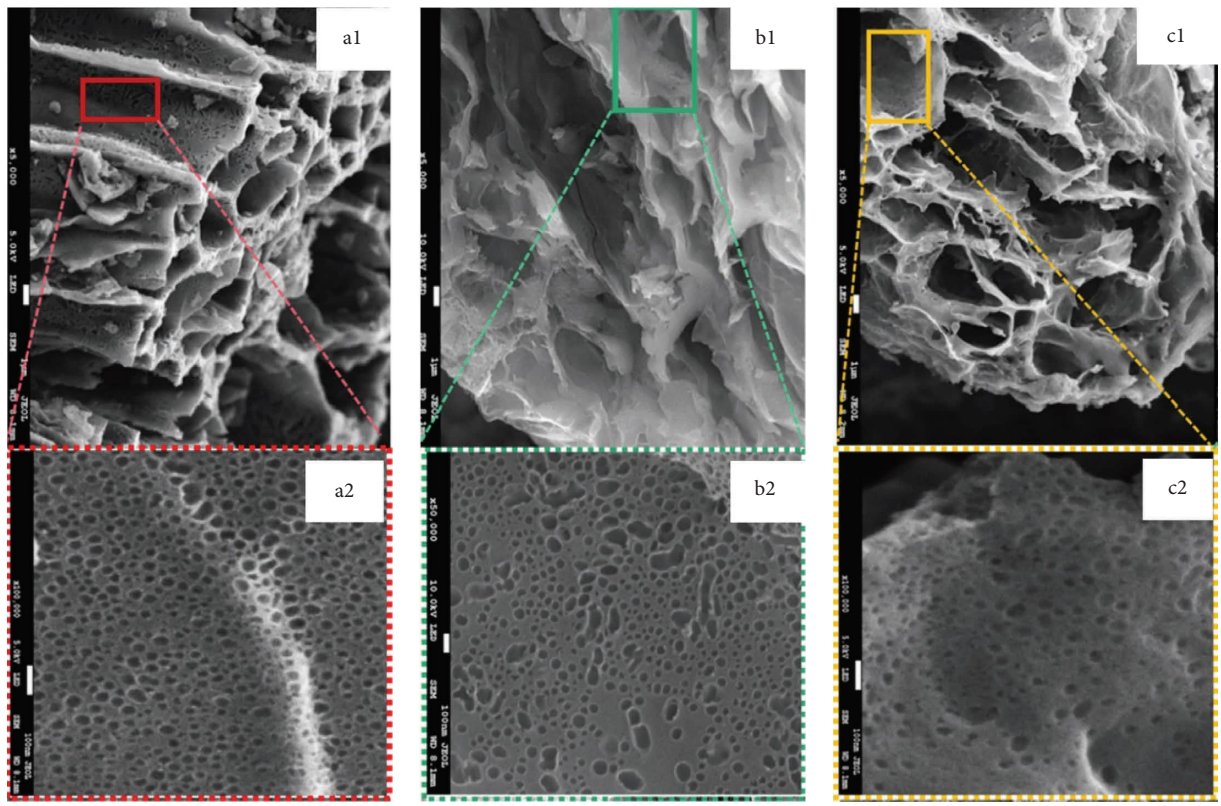

FIGURE 9: Scanning electron microscopy images taken at different resolutions: (a) (a1 and a2) for SPC-1, (b) (b1 and b2) for SPC-2, and (c) (c1 and c2) for SPC-3. Reprinted from [180] with Elsevier permission.

TABLE 4: Effect of pore distribution and specific surface area on electrochemical performance of porous carbon materials.

Carbon precursor	V_{micro} ($cm^3 \cdot g^{-1}$)	V_{meso} ($cm^3 \cdot g^{-1}$)	V_{micro}/V_{meso}	V_{tot} ($cm^3 \cdot g^{-1}$)	SSA ($m^2 \cdot g^{-1}$)	C_{SP} (Fg^{-1})	R_C (Ω)	Reference
Green tea	1.023	0.360	2.841	NR	1966	397 (5 mA/cm^2)	0.12	[85]
Wood tar	0.67	0.35	1.914	1.02	1898.86	338.5 (1 A/g)	0.1	[164]
Lignin	0.70	1.33	0.526	2.02	2866	216 (0.5 A/cm^2)	NR	[204]
Tea waste	0.5420	0.050	10.84	0.592	1125	203 (1.5 mA/m^2)	NR	[205]
Shaddock endothelium	0.583	0.135	4.318	0.746	1265	550 (0.2 A/g)	0.4	[161]
Coconut shells	0.44	1.06	0.415	1.50	2105	181.8 (0.1 A/g)	NR	[206]
Biomass-derived polyacrylonitrile	0.211	0.023	9.173	0.234	469	212 (0.5 mA/g)	0.51	[205]
Rice husk	1.132	0.639	1.771	1.771	3263	315 (0.5 A/g)	NR	[207]
Rice husk without silica	0.476	1.32	0.360	1.796	2804	278 (0.5 Ag)	NR	[207]
Sakura petals	0.55	0.23	2.391	0.78	1433.76	265.8 (0.2 A/g)	NR	[208]
Gulfweed	1.32	1.05	1.257	2.37	3155	395 (0.05 A/g)	NR	[209]
Cashew nut shells	0.28	0.09	3.111	0.46	898.3	214 (1 A/g)	NR	[170]
Coffee ground	1.337	2.461	0.543	3.797	3065	127.8 (1 A/g)	NR	[171]
Chestnut shells	0.65	0.41	1.585	1.09	1347.93	201 (0.5 A/g)	NR	[210]
Cotton	1.38	0.64	2.156	2.04	2743	279 (1 A/g)	0.63	[211]
Agaric	0.94	0.21	4.476	1.15	2225.5	374 (0.5 A/g)	0.6	[202]
Yeast-treated banana peel	0.26	0.16	1.625	NR	1084	476 (0.1 A/g)	NR	[212]
Poplar wood	0.45	0.48	0.937	0.93	1573.34	323 (0.5 A/g)	0.08	[213]
Sterculia lychnophora	0.79	0.36	2.194	1.15	1808	295 (1 A/g)	0.26	[201]
Bagasse	0.58	0.23	2.521	0.86	1892.4	142.1 (0.5 A/g)	NR	[203]

supercapacitors have a thickness between 100 μm and 200 μm with ~10mgcm^{-2} of active materials, while many of the investigations have utilized 5 – 15μm as electrode's thickness with 0.5 – 1mgcm^{-2} active materials [218]. Electrodes of 42μm and 185 μm thickness have achieved 196Fg^{-1} and 402mFcm^{-2}, respectively [219], demonstrating a decrease in C_{SP} as the electrode thickness increases, which limits the accessibility to the active sites within the electrode to electrolytes ions. The

volumetric capacitance of 100μm, 400μm, and 800μm electrodes decreased from 168Fcm^{-3} at 100μm to 82Fcm^{-3} at 800μm. The highest energy density was achieved by a 400μm electrode thickness material, which achieved 150Fcm^{-3} at 20mVs^{-1} as a result of a voltage scan [220]. A basswood-based electrode with a thickness of 800μm and 40mgcm^{-2} active materials has demonstrated a C_{SP} of 223.9Fg^{-1} at 0.05Ag^{-1} and a volumetric capacitance of 81.7Fcm^{-3} at 2mgcm^{-2}. Basswood-based electrodes produced an EDLC with a charge transfer resistance of 0.37 Ω and an energy density of 22.4Whkg^{-1} at a power density of 1996.4Wkg^{-1} [186]. The increase in the electrode thickness decreases C_{SP} and operating voltage while increasing the ESR, number of pores within the porous carbon-based electrodes, and cyclic stability [221].

3. Challenges and Opportunities in Biomass-Derived Porous Carbon-Based EDLC Electrodes

In the field of biomass as porous carbon precursors, many researchers emphasize the availability and low cost of biomass materials, often derived as waste from crop-harvesting processes. Additionally, some researchers target biomass based on their physical and elemental compositions, which can vary depending on the geographic location. Therefore, prescribing a general selection method for all biomass types is complex due to variations in harvesting methods across different crops. The synthesis of biomass-derived porous carbon involves numerous steps, parameters, and conditions that have a significant impact on the final product. Furthermore, different raw biomass resources have distinct physicochemical properties and different elemental compositions that affect steps, conditions, and parameters that must be considered during their conversion into porous carbon. Consequently, it is impossible to identify general conditions that are productive for all types of biomass used as carbon precursors.

The effect of average pore size diameter, structures and distribution, and SSA on the storage capacity of EDLCs has not been thoroughly investigated. Therefore, a comprehensive examination of the effect of pore size diameter, the ratio of micropores to mesopores, and SSA on the electrochemical properties of porous carbon-based electrodes for EDLCs is required. Various studies have reported contradictory information regarding the effect of activation time on the physicochemical and electrochemical properties of biomass-derived porous carbon, indicating that the effect of activation time remains unclear. Thus, a comprehensive and clear investigation into the effect of activation time on the physicochemical and electrochemical properties of AC-based electrode materials derived from biomass should be conducted. In addition, low electrical conductivity presented by biomass-derived porous carbon and controlling the pore size distribution of AC has become a significant challenge due to the dissimilar structure and chemical composition of biomass materials. Hence, there is a need for improved synthesis techniques that can contribute to a proper pore size structure and distribution within biomass-derived porous carbon materials, which could lead to an energy storage device with superior electrochemical performance.

Opportunities in this field include investigating the following: (1) The variation of the elemental composition of the same biomass grown from different locations geographically. (2) There is a need to investigate how modifying the heating rate and time during carbonization/activation influences the physicochemical and electrochemical properties of porous carbon materials. Understanding these effects will aid in optimizing the synthesis process and producing materials with desirable properties. (3) To determine the optimum micropore-to-mesopore ratio that will lead to a high and beneficial SSA, it is essential to investigate the ideal volume ratio of micropores to mesopores. This parameter plays an important role in determining the C_{SP} of the materials, which has a direct effect on their energy storage capacity. (4) It is crucial to examine and understand C_{SP}, energy density, and power density generated by biomass-derived porous carbon-based EDLC electrodes, which remain unclear. The current knowledge in this area is limited as the highest C_{SP} reported does not necessarily correspond to the highest energy density or power density. Thus, deep investigation in this field will be needed and must consider the findings of this review to produce biomass-derived porous carbon-based EDLC electrodes with the best electrochemical performance. Consequently, this review offers a guideline and will facilitate future researchers in the field to emphasize the needful and very crucial subjects in the field.

4. Conclusion

This review investigates the impact of synthesis techniques, operating conditions, and physicochemical properties on the electrochemical properties and performance of biomass-derived AC for EDLC electrodes. The review focuses on three primary factors: the initial properties of raw biomass as a carbon precursor, the operating conditions, and the physicochemical properties of the resultant biomass-derived porous carbon materials. Various synthesis techniques, activating agents, the mass ratio of activating agent to biomass, carbonization/activation time, operating temperature, mass of the active material in the electrode, and the thickness of the electrode are investigated as operating conditions. In addition, the physicochemical properties, such as surface morphology and surface functional groups, of the derived porous carbon were extensively evaluated and presented. Multiple factors influence the properties of porous carbon derived from biomass and the performance of the resultant electrodes. This review demonstrates that several parameters, conditions, and synthesis methods employed affect the properties of electrode materials. Due to the unique complexity of different biomass structures and their chemical composition, it is not easy to determine the right general activating agent and synthesis method. But, based on the reported results, we can recommend future researchers consider the N- and P-doping technique with chemical activation for the development of the porous structure of biomass-derived carbon materials.

The optimum mass ratio of the activating agent to the carbon precursor is highly dependent on the composition of the carbon precursors. The pore structure and distribution

have a substantial effect on the SSA and capacitance. Hence, the operating conditions have a significant effect on the physicochemical and electrochemical properties, as well as the performance of the biomass-derived porous carbon materials. Carbon-based electrodes exhibit pseudocapacitance behavior due to the enhancement of wettability by surface functional groups, which has a positive effect on the performance of the EDLCs. Finally, to improve the electrochemical performance of EDLC electrodes, a combination of factors must be considered rather than a single factor alone. Optimizing the properties and performance of biomass-derived porous carbon materials is dependent on the interplay between various parameters, conditions, and synthesis methodologies. Future works in this area are given as follows:

(a) Researchers should aim to investigate the effects of the operating conditions employed in the synthesis of biomass into porous carbon materials on their physicochemical properties.

(b) Future researchers should investigate practically the effect of various physicochemical properties of biomass-derived porous carbon on as-produced electrodes' performance for more clarification.

(c) Lastly, more attention should be focused on knowing the optimum parameters/conditions of physicochemical properties required to enhance EDLC electrodes' electrochemical performance.

Inclusive, future work should continue to investigate all possibilities to solve the abovementioned challenges, and it is recommended to consider the contribution of electrolyte materials in use. This review offers a guideline and will facilitate future researchers in the field to emphasize the needful and very crucial subjects in the field.

Data Availability

This manuscript is a review paper means that it combined and compared already published data. Therefore, as a review paper, all used data are from previous reported studies and datasets that have been cited in this study. Hence, for more information, you can check our bibliography or reference part or contact the corresponding author.

Conflicts of Interest

The authors declare that there are no conflicts of interest.

Authors' Contributions

C.A. wrote the first draft; A.B. and R.M. reviewed and edited the draft, and Y.A.C.J., R.M., and A.B. supervised the study. All authors have read and agreed to the submitted manuscript version.

Acknowledgments

This research was conducted as part of my Ph.D. studies that were supported by the Partnership for Skills in Applied, Engineering, and Technology (PASET)-Regional Scholarship and Innovation Fund (RSIF) with Project No. P165581. The authors acknowledge the Partnership for Skills in Applied, Engineering, and Technology (PASET)-Regional Scholarship and Innovation Fund (RSIF) for sponsoring the studies.

References

[1] S. Ould Amrouche, D. Rekioua, T. Rekioua, and S. Bacha, "Overview of energy storage in renewable energy systems," *International Journal of Hydrogen Energy*, vol. 41, no. 45, pp. 20914–20927, 2016.

[2] M. Baumann, M. Weil, J. F. Peters, N. Chibeles-Martins, and A. B. Moniz, "A review of multi-criteria decision making approaches for evaluating energy storage systems for grid applications," *Renewable and Sustainable Energy Reviews*, vol. 107, pp. 516–534, 2019.

[3] T. Terlouw, T. AlSkaif, C. Bauer, and W. Van Sark, "Multi-objective optimization of energy arbitrage in community energy storage systems using different battery technologies," *Applied Energy*, vol. 239, pp. 356–372, 2019.

[4] D. Wang, Z. Geng, B. Li, and C. Zhang, "High performance electrode materials for electric double-layer capacitors based on biomass-derived activated carbons," *Electrochimica Acta*, vol. 173, pp. 377–384, 2015.

[5] T. K. Enock, C. K. King'ondu, A. Pogrebnoi, and Y. A. C. Jande, "Status of biomass derived carbon materials for supercapacitor application," *International Journal of Electrochemistry*, vol. 2017, Article ID 6453420, 14 pages, 2017.

[6] S. Alipoori, S. Mazinani, S. H. Aboutalebi, and F. Sharif, "Review of PVA-based gel polymer electrolytes in flexible solid-state supercapacitors: opportunities and challenges," *Journal of Energy Storage*, vol. 27, Article ID 101072, 2020.

[7] Z. Bi, Q. Kong, Y. Cao et al., "Biomass-derived porous carbon materials with different dimensions for supercapacitor electrodes: a review," *Journal of Materials Chemistry A*, vol. 7, no. 27, pp. 16028–16045, Article ID 16028, 2019.

[8] M. Cakici, R. R. Kakarla, and F. Alonso-Marroquin, "Advanced electrochemical energy storage supercapacitors based on the flexible carbon fiber fabric-coated with uniform coral-like MnO2 structured electrodes," *Chemical Engineering Journal*, vol. 309, pp. 151–158, 2017.

[9] P. Chand and A. Joshi, "Biomass derived carbon for supercapacitor applications," *Journal of Energy Storage*, vol. 39, Article ID 102646, 2021.

[10] B. Dyatkin, V. Presser, M. Heon, M. R. Lukatskaya, M. Beidaghi, and Y. Gogotsi, "Development of a green supercapacitor composed entirely of environmentally friendly materials," *ChemSusChem*, vol. 6, no. 12, pp. 2269–2280, 2013.

[11] A. Cultura and Z. Salameh, "Modeling, evaluation and simulation of a supercapacitor module for energy storage application," *Cell*, vol. 1, no. 1, p. 1, 2015.

[12] Y. Wang, L. Zhang, H. Hou et al., "Recent progress in carbon-based materials for supercapacitor electrodes: a review," *Journal of Materials Science*, vol. 56, no. 1, pp. 173–200, 2020.

[13] A. Jain, Y. Ziai, K. Bochenek, S. R. Manippady, F. Pierini, and M. Michalska, "Utilization of compressible hydrogels as electrolyte materials for supercapacitor applications," *RSC Advances*, vol. 13, no. 17, pp. 11503–11512, 2023.

[14] A. Jain, M. Michalska, A. Zaszczyńska, and P. Denis, "Surface modification of activated carbon with silver

nanoparticles for electrochemical double layer capacitors," *Journal of Energy Storage*, vol. 54, Article ID 105367, 2022.
[15] L. Guardia, L. Suárez, N. Querejeta et al., "Biomass waste-carbon/reduced graphene oxide composite electrodes for enhanced supercapacitors," *Electrochimica Acta*, vol. 298, pp. 910–917, 2019.
[16] Z. S. Iro, C. Subramani, and S. Dash, "A brief review on electrode materials for supercapacitor," *International Journal of Electrochemical Science*, vol. 11, no. 12, pp. 10628–10643, 2016.
[17] N. M. Keppetipola, C. Olivier, T. Toupance, and L. Cojocaru, "Biomass-derived carbon electrodes for supercapacitors and hybrid solar cells: towards sustainable photo-supercapacitors," *Sustainable Energy Fuels*, vol. 5, no. 19, pp. 4784–4806, 2021.
[18] L. Lyu, K.-D. Seong, D. Ko et al., "Recent development of biomass-derived carbons and composites as electrode materials for supercapacitors," *Materials Chemistry Frontiers*, vol. 3, no. 12, pp. 2543–2570, 2019.
[19] S. Mishra, R. Srivastava, A. Muhammad et al., "The impact of physicochemical features of carbon electrodes on the capacitive performance of supercapacitors: a machine learning approach," 2022, https://arxiv.org/abs/2208.04172.
[20] S. Najib and E. Erdem, "Current progress achieved in novel materials for supercapacitor electrodes: mini review," *Nanoscale Advances*, vol. 1, no. 8, pp. 2817–2827, 2019.
[21] M. D. Stoller and R. S. Ruoff, "Best practice methods for determining an electrode material's performance for ultracapacitors," *Energy and Environmental Science*, vol. 3, no. 9, p. 1294, 2010.
[22] S. Rajeevan, S. John, and S. C. George, "Polyvinylidene fluoride: a multifunctional polymer in supercapacitor applications," *Journal of Power Sources*, vol. 504, Article ID 230037, 2021.
[23] L. Lai, H. Yang, L. Wang et al., "Preparation of supercapacitor electrodes through selection of graphene surface functionalities," *ACS Nano Journal*, vol. 6, no. 7, pp. 5941–5951, 2012.
[24] Z. Yu, L. Tetard, L. Zhai, and J. Thomas, "Supercapacitor electrode materials: nanostructures from 0 to 3 dimensions," *Energy and Environmental Science*, vol. 8, no. 3, pp. 702–730, 2015.
[25] M. A. Azam, N. S. N. Ramli, N. A. N. M. Nor, and T. I. T. Nawi, "Recent advances in biomass-derived carbon, mesoporous materials, and transition metal nitrides as new electrode materials for supercapacitor: a short review," *International Journal of Energy Research*, vol. 45, no. 6, pp. 8335–8346, 2021.
[26] J. Chaparro-Garnica, D. Salinas-Torres, M. J. Mostazo-López, E. Morallón, and D. Cazorla-Amorós, "Biomass waste conversion into low-cost carbon-based materials for supercapacitors: a sustainable approach for the energy scenario," *Journal of Electroanalytical Chemistry*, vol. 880, Article ID 114899, 2021.
[27] J.-H. Choi, C. Lee, S. Cho et al., "High capacitance and energy density supercapacitor based on biomass-derived activated carbons with reduced graphene oxide binder," *Carbon*, vol. 132, pp. 16–24, 2018.
[28] B. K. Kim, S. Sy, A. Yu, and J. Zhang, "Electrochemical supercapacitors for energy storage and conversion," *Handbook of Clean Energy Systems*, vol. 5, pp. 1–25, 2015.
[29] P. Dubey, V. Shrivastav, P. H. Maheshwari, and S. Sundriyal, "Recent advances in biomass derived activated carbon electrodes for hybrid electrochemical capacitor applications: challenges and opportunities," *Carbon*, vol. 170, pp. 1–29, 2020.
[30] R. Raccichini, A. Varzi, S. Passerini, and B. Scrosati, "The role of graphene for electrochemical energy storage," *Nature Materials*, vol. 14, no. 3, pp. 271–279, 2015.
[31] K. Moses, K. Richard, O. Kingsley et al., "Porous carbon derived from Zea mays cobs as excellent electrodes for supercapacitor applications," *Open Journal of Analytical and Bioanalytical Chemistry*, vol. 7, no. 1, pp. 001–10, 2023.
[32] A. Bello, N. Manyala, F. Barzegar, A. A. Khaleed, D. Y. Momodu, and J. K. Dangbegnon, "Renewable pine cone biomass derived carbon materials for supercapacitor application," *RSC Advances*, vol. 6, no. 3, pp. 1800–9, 2016.
[33] Z. Li, D. Guo, Y. Liu, H. Wang, and L. Wang, "Recent advances and challenges in biomass-derived porous carbon nanomaterials for supercapacitors," *Chemical Engineering Journal*, vol. 397, Article ID 125418, 2020.
[34] S. Y. Lu, M. Jin, Y. Zhang, Y. B. Niu, J. C. Gao, and C. M. Li, "Chemically exfoliating biomass into a graphene-like porous active carbon with rational pore structure, good conductivity, and large surface area for high-performance supercapacitors," *Advanced Energy Materials*, vol. 8, no. 11, Article ID 1702545, 2018.
[35] T. Yumak, G. A. Yakaboylu, O. Oginni, K. Singh, E. Ciftyurek, and E. M. Sabolsky, "Comparison of the electrochemical properties of engineered switchgrass biomass-derived activated carbon-based EDLCs," *Colloids and Surfaces A: Physicochemical and Engineering Aspects*, vol. 586, Article ID 124150, 2020.
[36] Q. Abbas, M. Mirzaeian, A. A. Ogwu, M. Mazur, and D. Gibson, "Effect of physical activation/surface functional groups on wettability and electrochemical performance of carbon/activated carbon aerogels based electrode materials for electrochemical capacitors," *International Journal of Hydrogen Energy*, vol. 45, no. 25, pp. 13586–95, 2020.
[37] F. Lin, X. Liu, M. Ma et al., "Real-time monitoring the carbonization and activation process of activated carbon prepared from Chinese parasol via zinc chloride activation," *Journal of Analytical and Applied Pyrolysis*, vol. 155, Article ID 105089, 2021.
[38] N. Díez, M. Sevilla, A. Fombona-Pascual, and A. .B Fuertes, "Monodisperse porous carbon nanospheres with ultra-high surface area for energy storage in electrochemical capacitors," *Batteries and Supercaps*, vol. 5, no. 3, Article ID e202100169, 2022.
[39] T. K. Enock, C. K. King'ondu, A. Pogrebnoi, and Y. A. C. Jande, "Biogas-slurry derived mesoporous carbon for supercapacitor applications," *Materials Today Energy*, vol. 5, pp. 126–37, 2017.
[40] K. Sirengo, Y. Jande, T. E. Kibona, A. Hilonga, C. Muiva, and C. K. King'ondu, "Fish bladder-based activated carbon/Co3O4/TiO2 composite electrodes for supercapacitors," *Materials Chemistry and Physics*, vol. 232, pp. 49–56, 2019.
[41] H. Krishnamoorthy, R. Ramyea, A. Maruthu, K. Kandasamy, M. Michalska, and S. K. Kandasamy, "Synthesis methods of carbonaceous materials from different bio-wastes as electrodes for supercapacitor and its electrochemistry-A review," *Bioresource Technology Reports*, vol. 19, Article ID 101187, 2022.
[42] S. Mohammad, S. Ahmed, A. Badawi, and D. El-Desouki, "Activated carbon derived from egyptian banana peels for removal of cadmium from water," *Journal of Applied Life Sciences International*, vol. 3, no. 2, pp. 77–88, 2015.

[43] M. Alzaid, F. Alsalh, and M. Z. Iqbal, "Biomass derived activated carbon based hybrid supercapacitors," *Journal of Energy Storage*, vol. 40, Article ID 102751, 2021.
[44] M. Gao, C.-C. Shih, S.-Y. Pan, C.-C. Chueh, and W.-C. Chen, "Advances and challenges of green materials for electronics and energy storage applications: from design to end-of-life recovery," *Journal of Materials Chemistry A*, vol. 6, no. 42, 2018.
[45] S. Jung, Y. Myung, B. N. Kim, I. G. Kim, I.-K. You, and T. Kim, "Activated biomass-derived graphene-based carbons for supercapacitors with high energy and power density," *Scientific Reports*, vol. 8, no. 1, pp. 1915–8, 2018.
[46] T. Li, R. Ma, J. Lin et al., "The synthesis and performance analysis of various biomass-based carbon materials for electric double-layer capacitors: A review," *International Journal of Energy Research*, vol. 44, no. 4, pp. 2426–54, 2019.
[47] W. Lu, Y. Si, C. Zhao et al., "Biomass-derived carbon applications in the field of supercapacitors: Progress and prospects," *Chemical Engineering Journal*, vol. 495, Article ID 153311, 2024.
[48] S. Sagadevan, T. Balakrishnan, M. Z. Rahman et al., "Agricultural biomass-based activated carbons for efficient and sustainable supercapacitors," *Journal of Energy Storage*, vol. 97, Article ID 112878, 2024.
[49] D. Balasubramanian, H. Varadharajan, I. Papla Venugopal, and E. G. Varuvel, "Recent advances and research progress on the role of carbon-based biomass in ultra-capacitors: A systematic review," *Energy Storage*, vol. 6, no. 4, p. e646, 2024.
[50] M. Sk, P. Pradhan, B. Patra, and A. Guria, "Green biomass derived porous carbon materials for electrical double-layer capacitors (EDLCs)," *Materials Today Chemistry*, vol. 30, Article ID 101582, 2023.
[51] X. Luo, S. Chen, T. Hu, Y. Chen, and F. Li, "Renewable biomass-derived carbons for electrochemical capacitor applications," *Sustainable Materials and Technologies*, vol. 1, no. 2, pp. 211–40, 2021.
[52] D. S. Priya, L. J. Kennedy, and G. T. Anand, "Emerging trends in biomass-derived porous carbon materials for energy storage application: A critical review," *Materials Today Sustainability*, vol. 21, Article ID 100320, 2023.
[53] C. Yuan, H. Xu, S. A El-khodary et al., "Recent advances and challenges in biomass-derived carbon materials for supercapacitors: A review," *Fuel*, vol. 362, Article ID 130795, 2024.
[54] H. Zhang, Y. Zhang, L. Bai, Y. Zhang, and L. Sun, "Effect of physiochemical properties in biomass-derived materials caused by different synthesis methods and their electrochemical properties in supercapacitors," *Journal of Materials Chemistry A*, vol. 9, no. 21, pp. 12521–52, 2021.
[55] S. S. Shah, M. A. Aziz, M. Ali et al., "Future directions and challenges in biomass-based supercapacitors. biomass-based supercapacitors: design," *Fabrication and Sustainability*, vol. 26, pp. 461–83, 2023.
[56] L. Liang, L. Li, R. Chen et al., "Research advances in plant-derived activated carbon for electric double layer capacitors," *Journal of Alloys and Compounds*, vol. 992, Article ID 174641, 2024.
[57] L. Sun, Y. Gong, D. Li, and C. Pan, "Biomass-derived porous carbon materials: synthesis, designing, and applications for supercapacitors," *Green Chemistry*, vol. 24, no. 10, pp. 3864–94, 2022.
[58] E. Redondo, J. Carretero-González, E. Goikolea, J. Ségalini, and R. Mysyk, "Effect of pore texture on performance of activated carbon supercapacitor electrodes derived from olive pits," *Electrochimica Acta*, vol. 160, pp. 178–84, 2015.
[59] Y. Cao, X. Wang, Z. Gu et al., "Potassium chloride templated carbon preparation for supercapacitor," *Journal of Power Sources*, vol. 384, pp. 360–6, 2018.
[60] R. Heimböckel, F. Hoffmann, and M. Fröba, "Insights into the influence of the pore size and surface area of activated carbons on the energy storage of electric double layer capacitors with a new potentially universally applicable capacitor model," *Physical Chemistry Chemical Physics*, vol. 21, no. 6, pp. 3122–33, 2019.
[61] C. Liu, F. Li, L. P. Ma, and H. M. Cheng, "Advanced materials for energy storage," *Advanced Materials*, vol. 22, no. 8, pp. E28–62, 2010.
[62] S. Sundriyal, V. Shrivastav, H. D. Pham, S. Mishra, A. Deep, and D. P. Dubal, "Advances in bio-waste derived activated carbon for supercapacitors: Trends, challenges and prospective," *Resources, Conservation and Recycling*, vol. 169, Article ID 105548, 2021.
[63] C. Zhang, Z. Geng, M. Cai et al., "Microstructure regulation of super activated carbon from biomass source corncob with enhanced hydrogen uptake," *International Journal of Hydrogen Energy*, vol. 38, no. 22, pp. 9243–50, 2013.
[64] M. Nazhipkyzy, M. Yeleuov, S. T. Sultakhan et al., "Electrochemical Performance of Chemically Activated Carbons from Sawdust as Supercapacitor Electrodes," *Nanomaterials*, vol. 12, no. 19, p. 3391, 2022.
[65] D. Momodu, M. Madito, F. Barzegar et al., "Activated carbon derived from tree bark biomass with promising material properties for supercapacitors," *Journal of Solid State Electrochemistry*, vol. 21, no. 3, pp. 859–72, 2017.
[66] M. P. Chavhan, V. Slovak, G. Zelenkova, and D. Dominko, "Revisiting the effect of pyrolysis temperature and type of activation on the performance of carbon electrodes in an electrochemical capacitor," *Materials*, vol. 15, no. 7, p. 2431, 2022.
[67] L. Jiang, J. Yan, L. Hao, R. Xue, G. Sun, and B. Yi, "High rate performance activated carbons prepared from ginkgo shells for electrochemical supercapacitors," *Carbon*, vol. 56, pp. 146–54, 2013.
[68] O. Fasakin, J. K. Dangbegnon, D. Y. Momodu et al., "Synthesis and characterization of porous carbon derived from activated banana peels with hierarchical porosity for improved electrochemical performance," *Electrochimica Acta*, vol. 262, pp. 187–96, 2018.
[69] K. Dujearic-Stephane, P. Panta, Y. M. Shulga, A. Kumar, M. Gupta, and Y. Kumar, "Physico-chemical characterization of activated carbon synthesized from Datura metel's peels and comparative capacitive performance analysis in acidic electrolytes and ionic liquids," *Bioresource Technology Reports*, vol. 11, Article ID 100516, 2020.
[70] A. Jain, M. Ghosh, M. Krajewski, S. Kurungot, and M. Michalska, "Biomass-derived activated carbon material from native European deciduous trees as an inexpensive and sustainable energy material for supercapacitor application," *Journal of Energy Storage*, vol. 34, Article ID 102178, 2021.
[71] K. Wang, N. Zhao, S. Lei et al., "Promising biomass-based activated carbons derived from willow catkins for high performance supercapacitors," *Electrochimica Acta*, vol. 166, pp. 1–11, 2015.
[72] Q. Sun, T. Jiang, J. Shi, and G. Zhao, "Porous carbon material based on biomass prepared by MgO template method and ZnCl2 activation method as electrode for high performance

supercapacitor," *International Journal of Electrochemical Science*, vol. 14, no. 1, pp. 1–14, 2019.

[73] T. N. Nguyen, P. A. Le, and V. B. T. Phung, "Facile green synthesis of carbon quantum dots and biomass-derived activated carbon from banana peels: synthesis and investigation," *Biomass Conversion and Biorefinery*, vol. 12, no. 7, pp. 2407–16, 2020.

[74] K. Ning, G. Zhao, H. Liu et al., "N and S co-doped 3D hierarchical porous carbon as high-performance electrode material for supercapacitors," *Diamond and Related Materials*, vol. 126, Article ID 109080, 2022.

[75] X. Liang, R. Liu, and X. Wu, "Biomass waste derived functionalized hierarchical porous carbon with high gravimetric and volumetric capacitances for supercapacitors," *Microporous and Mesoporous Materials*, vol. 310, Article ID 110659, 2021.

[76] L. Wang, X. Li, X. Huang, S. Han, and J. Jiang, "Activated green resources to synthesize N, P co-doped O-rich hierarchical interconnected porous carbon for high-performance supercapacitors," *Journal of alloys and compounds*, vol. 891, Article ID 161908, 2022.

[77] M. Karnan, K. Hari Prakash, and S. Badhulika, "Revealing the super capacitive performance of N-doped hierarchical porous activated carbon in aqueous, ionic liquid, and redox additive electrolytes," *Journal of Energy Storage*, vol. 53, Article ID 105189, 2022.

[78] A. Gopalakrishnan, T. D. Raju, and S. Badhulika, "Green synthesis of nitrogen, sulfur-co-doped worm-like hierarchical porous carbon derived from ginger for outstanding supercapacitor performance," *Carbon (New York)*, vol. 168, pp. 209–19, 2020.

[79] L. Luo, Y. Zhou, W. Yan, X. Wu, S. Wang, and W. Zhao, "Two-step synthesis of B and N co-doped porous carbon composites by microwave-assisted hydrothermal and pyrolysis process for supercapacitor application," *Electrochimica Acta*, vol. 360, Article ID 137010, 2020.

[80] S. Kong, X. Xiang, B. Jin et al., "B, O and N codoped biomass-derived hierarchical porous carbon for high-performance electrochemical energy storage," *Nanomaterials*, vol. 12, no. 10, p. 1720, 2022.

[81] A. Wang, K. Sun, R. Xu, Y. Sun, and J. Jiang, "Cleanly synthesizing rotten potato-based activated carbon for supercapacitor by self-catalytic activation," *Journal of Cleaner Production*, vol. 283, Article ID 125385, 2021.

[82] L. Hu, Q. Zhu, Q. Wu, D. Li, Z. An, and B. Xu, "Natural biomass-derived hierarchical porous carbon synthesized by an in situ hard template coupled with NAOH activation for ultrahigh rate supercapacitors," *ACS Sustainable Chemistry & Engineering*, vol. 6, no. 11, pp. 13949–59, 2018.

[83] D. Shrestha and A. Rajbhandari, "The effects of different activating agents on the physical and electrochemical properties of activated carbon electrodes fabricated from wood-dust of Shorea robusta," *Heliyon*, vol. 7, no. 9, Article ID e07917, 2021.

[84] C. Wang, D. Wu, H. Wang, Z. Gao, F. Xu, and K. Jiang, "Biomass derived nitrogen-doped hierarchical porous carbon sheets for supercapacitors with high performance," *Journal of Colloid snd Interface Science*, vol. 523, pp. 133–43, 2018.

[85] D. Gandla, H. Chen, and D. Q. Tan, "Mesoporous structure favorable for high voltage and high energy supercapacitor based on green tea waste-derived activated carbon," *Materials research express*, vol. 7, no. 8, Article ID 85606, 2020.

[86] A. Elmouwahidi, E. Bailón-García, L. A. Romero-Cano, A. I. Zárate-Guzmán, A. F. Pérez-Cadenas, and F. Carrasco-Marín, "Influence of surface chemistry on the electrochemical performance of biomass-derived carbon electrodes for its use as supercapacitors," *Materials*, vol. 12, no. 15, p. 2458, 2019.

[87] V. Gehrke, G. K. Maron, L. da Silva Rodrigues et al., "Facile preparation of a novel biomass-derived H_3PO_4 and Mn $(NO_3)_2$ activated carbon from citrus bergamia peels for high-performance supercapacitors," *Materials Today Communications*, vol. 26, Article ID 101779, 2021.

[88] M. Vinayagam, R. Suresh Babu, A. Sivasamy, and A. L. Ferreira de Barros, "Biomass-derived porous activated carbon from Syzygium cumini fruit shells and Chrysopogon zizanioides roots for high-energy density symmetric supercapacitors," *Biomass and Bioenergy*, vol. 143, Article ID 105838, 2020.

[89] R. Khayyam Nekouei, S. Mofarah, S. Maroufi, W. Wang, I. Mansuri, and V. Sahajwalla, "Unraveling the role of oxides in electrochemical performance of activated carbons for high voltage symmetric electric double-layer capacitors," *Advanced Energy and Sustainability Research*, vol. 3, no. 1, Article ID 2100130, 2021.

[90] C. Xia and S. Q. Shi, "Self-activation for activated carbon from biomass: theory and parameters," *Green Chemistry*, vol. 18, no. 7, pp. 2063–71, 2016.

[91] B. Lesbayev, M. Auyelkhankyzy, G. Ustayeva et al., "Modification of biomass-derived nanoporous carbon with nickel oxide nanoparticles for supercapacitor application," *Journal of Composites Science*, vol. 7, no. 1, p. 20, 2023.

[92] S. J. Kim, B. C. Bai, M. I. Kim, and Y.-S. Lee, "Improved specific capacitance of pitch-based activated carbon by KOH/KMnO 4 agent for supercapacitors," *Carbon Letters*, vol. 30, no. 5, pp. 585–91, 2020.

[93] R. Nasser, J. Tiantian, and J.-M. Song, "Hierarchical porous activated carbon derived from olives: Preparation, (N, S) co-doping, and its application in supercapacitors," *Journal of Energy Storage*, vol. 51, Article ID 104348, 2022.

[94] H. Zhou, Y. Zhan, F. Guo et al., "Synthesis of biomass-derived carbon aerogel/MnOx composite as electrode material for high-performance supercapacitors," *Electrochimica Acta*, vol. 390, p. 1, 2021.

[95] K. Wiedner, C. Rumpel, C. Steiner, A. Pozzi, R. Maas, and B. Glaser, "Chemical evaluation of chars produced by thermochemical conversion (gasification, pyrolysis and hydrothermal carbonization) of agro-industrial biomass on a commercial scale," *Biomass and Bioenergy*, vol. 59, pp. 264–78, 2013.

[96] A. Bello, J. Dangbegnon, D. Y. Momodu, F. Ochai-Ejeh, K. O. Oyedotun, and N. Manyala, "Green and scalable synthesis of 3D porous carbons microstructures as electrode materials for high rate capability supercapacitors," *RSC Advances*, vol. 8, no. 71, pp. 40950–61, 2018.

[97] F. Cheng, H. Luo, L. Hu, B. Yu, Z. Luo, and M. Fidalgo de Cortalezzi, "Sludge carbonization and activation: From hazardous waste to functional materials for water treatment," *Journal of Environmental Chemical Engineering*, vol. 4, no. 4, pp. 4574–86, 2016.

[98] M. Amer and A. Elwardany, "Biomass carbonization. renewable energy-resources, challenges and applications," *IntechOpen*, vol. 7, 2020.

[99] I. Yang, M. Jung, M.-S. Kim, D. Choi, and J. C. Jung, "Physical and chemical activation mechanisms of carbon

materials based on the microdomain model," *Journal of Materials Chemistry A*, vol. 9, no. 15, pp. 9815–25, 2021.
[100] V. Jiménez, P. Sánchez, J. L. Valverde, and A. Romero, "Effect of the nature the carbon precursor on the physicochemical characteristics of the resulting activated carbon materials," *Materials Chemistry and Physics*, vol. 124, no. 1, pp. 223–33, 2010.
[101] W. Cao, "Biomass-derived activated carbons for electrical double layer supercapacitors: performance and stress effect," 2019, https://uknowledge.uky.edu/cme_etds/97/.
[102] R. Chakraborty, K. Vilya, M. Pradhan, and A. K. Nayak, "Recent advancement of biomass-derived porous carbon based materials for energy and environmental remediation applications," *Journal of Materials Chemistry A*, vol. 10, no. 13, pp. 6965–7005, 2022.
[103] S. De, A. M. Balu, J. C. van der Waal, and R. Luque, "Biomass-derived porous carbon materials: synthesis and catalytic applications," *ChemCatChem*, vol. 7, no. 11, pp. 1608–29, 2015.
[104] J. Akpa and K. Dagde, "Effect of activation method and agent on the characterization of prewinkle shell activated carbon," *Process Engineering*, vol. 56, pp. 24–36, 2018.
[105] D. Bergna, T. Varila, H. Romar, and U. Lassi, "Activated carbon from hydrolysis lignin: Effect of activation method on carbon properties," *Biomass and Bioenergy*, vol. 159, Article ID 106387, 2022.
[106] R. Lee, C. H. Kwak, H. Lee, S. Kim, and Y.-S. Lee, "Effect of nitrogen plasma surface treatment of rice husk-based activated carbon on electric double-layer capacitor performance," *Applied Chemistry for Engineering*, vol. 33, no. 1, pp. 71–7, 2022.
[107] Y. Gao, Q. Yue, B. Gao, and A. Li, "Insight into activated carbon from different kinds of chemical activating agents: A review," *Science of the Total Environment*, vol. 746, Article ID 141094, 2020.
[108] S. Kang, X. Li, J. Fan, and J. Chang, "Characterization of hydrochars produced by hydrothermal carbonization of lignin, cellulose, D-xylose, and wood meal," *Industrial & engineering chemistry research*, vol. 51, no. 26, pp. 9023–31, 2012.
[109] M. Siva Sankari and S. Vivekanandhan, "Jatropha oil cake based activated carbon for symmetric supercapacitor application: a comparative study on conventional and hydrothermal carbonization processes," *ChemistrySelect*, vol. 5, no. 4, pp. 1375–84, 2020.
[110] N. Manyala, A. Bello, F. Barzegar, A. A. Khaleed, D. Y. Momodu, and J. K. Dangbegnon, "Coniferous pine biomass: A novel insight into sustainable carbon materials for supercapacitors electrode," *Materials Chemistry and Physics*, vol. 182, pp. 139–47, 2016.
[111] M.-M. Titirici, R. J. White, C. Falco, and M. Sevilla, "Black perspectives for a green future: hydrothermal carbons for environment protection and energy storage," *Energy & Environmental Science.*, vol. 5, no. 5, pp. 6796–822, 2012.
[112] Y. Wu, J.-P. Cao, X.-Y. Zhao et al., "High-performance electrode material for electric double-layer capacitor based on hydrothermal pre-treatment of lignin by ZnCl2," *Applied Surface Science*, vol. 508, Article ID 144536, 2020.
[113] Y. Wu, J.-P. Cao, X.-Y. Zhao et al., "Preparation of porous carbons by hydrothermal carbonization and KOH activation of lignite and their performance for electric double layer capacitor," *Electrochimica Acta*, vol. 252, pp. 397–407, 2017.
[114] H. A. Hamouda, S. Cui, X. Dai et al., "Synthesis of porous carbon material based on biomass derived from hibiscus sabdariffa fruits as active electrodes for high-performance symmetric supercapacitors," *RSC Advances*, vol. 11, no. 1, pp. 354–63, 2021.
[115] U. I. Nda-Umar, I. Ramli, E. N. Muhamad, Y. H. Taufiq-Yap, and N. Azri, "Synthesis and characterization of sulfonated carbon catalysts derived from biomass waste and its evaluation in glycerol acetylation," *Biomass Conversion and Biorefinery*, vol. 12, no. 6, pp. 2045–2060, 2020.
[116] H. Yang, D. Zhang, Y. Chen, M Ran, and J. Gu, "Study on the application of KOH to produce activated carbon to realize the utilization of distiller's grains," in *Proceedings of the IOP Conference Series: Earth and Environmental Science*, IOP Publishing, Bristol, UK, June 2017.
[117] M. He, Z. Xu, Y. Sun, P. Chan, I. Lui, and D. C. Tsang, "Critical impacts of pyrolysis conditions and activation methods on application-oriented production of wood waste-derived biochar," *Bioresource Technology*, vol. 341, Article ID 125811, 2021.
[118] S. K. Kandasamy, R. Ravindaran, M. Michalska et al., "Highly carbonized Prunus dulcis shell-derived activated carbon for high-performance supercapacitor applications," *Polymer Bulletin*, vol. 80, no. 10, pp. 10881–10894, 2022.
[119] F. Wang, L. Chen, H. Li et al., "N-doped honeycomb-like porous carbon towards high-performance supercapacitor," *Chinese Chemical Letters*, vol. 31, no. 7, pp. 1986–90, 2020.
[120] S. K. Kandasamy, R. Ramyea, C. Arumugam et al., "Highly carbonized, porous activated carbon derived from ziziphus jujuba for energy storage," in *Proceedings of the International Conference on Advances in Energy Research*, Springer, Mumbai, India, July 2022.
[121] T. E. Rufford, D. Hulicova-Jurcakova, K. Khosla, Z. Zhu, and G. Q. Lu, "Microstructure and electrochemical double-layer capacitance of carbon electrodes prepared by zinc chloride activation of sugar cane bagasse," *Journal of Power Sources*, vol. 195, no. 3, pp. 912–8, 2010.
[122] R. Farma, S. F. Maurani, I. Apriyani, A. S. Rini, and A. S. Rini, "Fabrication of carbon electrodes from sago midrib biomass with chemical variation for supercapacitor cell application," *Journal of Physics: Conference Series*, vol. 2049, no. 1, 2021.
[123] G. Duan, L. Zhao, L. Chen et al., "ZnCl 2 regulated flax-based porous carbon fibers for supercapacitors with good cycling stability," *New Journal of Chemistry*, vol. 45, no. 48, pp. 22602–9, 2021.
[124] E. Gul, S. A. Shah, and S. N. A. Shah, "Chloride salt-activated carbon for supercapacitors," *Biomass-Based Supercapacitors: Design, Fabrication and Sustainability*, vol. 11, pp. 179–200, 2023.
[125] R. Machunda, H. Jeon, J. Lee, and J. Lee, "Effects of acid treatment on the improvement of specific capacitance and deionization efficiency of porous carbon electrodes," *Water Supply*, vol. 9, no. 2, pp. 159–65, 2009.
[126] S. Guo, B. Guo, R. Ma, Y. Zhu, and J. Wang, "KOH activation of coal-derived microporous carbons for oxygen reduction and supercapacitors," *RSC Advances*, vol. 10, no. 27, pp. 15707–14, 2020.
[127] N. Sinan and E. Unur, "Hydrothermal conversion of lignocellulosic biomass into high-value energy storage materials," *Journal of Energy Chemistry*, vol. 26, no. 4, pp. 783–9, 2017.
[128] S. Song, F. Ma, G. Wu, D. Ma, W. Geng, and J. Wan, "Facile self-templating large scale preparation of biomass-derived 3D hierarchical porous carbon for advanced

supercapacitors," *Journal of materials chemistry A*, vol. 3, no. 35, pp. 18154–62, 2015.

[129] C. Leng and K. Sun, "The preparation of 3D network pore structure activated carbon as an electrode material for supercapacitors with long-term cycle stability," *RSC Advances*, vol. 6, no. 62, pp. 57075–83, 2016.

[130] O. Togibasa, M. Mumfaijah, Y. K. Allo, K. Dahlan, and Y. O. Ansanay, "The effect of chemical activating agent on the properties of activated carbon from sago waste," *Applied Sciences*, vol. 11, no. 24, Article ID 11640, 2021.

[131] L. Wang, G. Mu, C. Tian et al., "Porous graphitic carbon nanosheets derived from cornstalk biomass for advanced supercapacitors," *ChemSusChem*, vol. 6, no. 5, pp. 880–9, 2013.

[132] J. P. Paraknowitsch and A. Thomas, "Doping carbons beyond nitrogen: an overview of advanced heteroatom doped carbons with boron, sulphur and phosphorus for energy applications," *Energy & Environmental Science.*, vol. 6, no. 10, pp. 2839–55, 2013.

[133] S. Uppugalla, U. Male, and P. Srinivasan, "Design and synthesis of heteroatoms doped carbon/polyaniline hybrid material for high performance electrode in supercapacitor application," *Electrochimica Acta*, vol. 146, pp. 242–8, 2014.

[134] D.-Y. Shin, K.-W. Sung, and H.-J. Ahn, "Synergistic effect of heteroatom-doped activated carbon for ultrafast charge storage kinetics," *Applied Surface Science*, vol. 478, pp. 499–504, 2019.

[135] A. Gopalakrishnan and S. Badhulika, "Effect of self-doped heteroatoms on the performance of biomass-derived carbon for supercapacitor applications," *Journal of Power Sources*, vol. 480, Article ID 228830, 2020.

[136] L. Cao, H. Li, X. Liu et al., "Nitrogen, sulfur co-doped hierarchical carbon encapsulated in graphene with "sphere-in-layer" interconnection for high-performance supercapacitor," *Journal of Colloid and Interface Science*, vol. 599, pp. 443–52, 2021.

[137] S. Zhang, K. Tian, B.-H. Cheng, and H. Jiang, "Preparation of N-doped supercapacitor materials by integrated salt templating and silicon hard templating by pyrolysis of biomass wastes," *ACS Sustainable Chemistry & Engineering*, vol. 5, no. 8, pp. 6682–91, 2017.

[138] J. Chen, Y Lin, J. Liu et al., "Outstanding supercapacitor performance of nitrogen-doped activated carbon derived from shaddock peel," *Journal of Energy Storage*, vol. 39, Article ID 102640, 2021.

[139] G. Hasegawa, T. Deguchi, K. Kanamori et al., "High-level doping of nitrogen, phosphorus, and sulfur into activated carbon monoliths and their electrochemical Capacitances," *Chemistry of Materials*, vol. 27, no. 13, pp. 4703–12, 2015.

[140] J. Han, Y. Ping, J. Li et al., "One-step nitrogen, boron codoping of porous carbons derived from pomelo peels for supercapacitor electrode materials," *Diamond and Related Materials*, vol. 96, pp. 176–81, 2019.

[141] S. Miao, K. Liang, J. Zhu, B. Yang, D. Zhao, and B. Kong, "Hetero-atom-doped carbon dots: doping strategies, properties and applications," *Nano Today*, vol. 33, Article ID 100879, 2020.

[142] M. P. Chavhan, D. Basu, A. Singh, and S. Ganguly, "N-doping in precursor sol: some observations in reference to in situ-grown carbon film electrodes for supercapacitor applications," *Energy Technology*, vol. 8, no. 5, Article ID 1901479, 2020.

[143] J. Li, K. Han, D. Wang et al., "Fabrication of high performance structural N-doped hierarchical porous carbon for supercapacitors," *Carbon*, vol. 164, pp. 42–50, 2020.

[144] S. N. A. Shah, E. Gul, N. C. D. Nath, and G. Du, "Biomass-derived N-doped carbon for electrochemical supercapacitors," *Biomass-Based Supercapacitors: Design, Fabrication and Sustainability*, vol. 17, pp. 289–313, 2023.

[145] H. Liu, M. Wang, D. D. Zhai, X. Y. Chen, and Z. J. Zhang, "Design and theoretical study of carbon-based supercapacitors especially exhibiting superior rate capability by the synergistic effect of nitrogen and phosphor dopants," *Carbon*, vol. 155, pp. 223–32, 2019.

[146] X. Xin, H. Kang, J. Feng et al., "A novel sol-gel strategy for N, P dual-doped mesoporous carbon with high specific capacitance and energy density for advanced supercapacitors," *Chemical Engineering Journal*, vol. 393, Article ID 124710, 2020.

[147] W. Ma, L. Xie, L. Dai et al., "Influence of phosphorus doping on surface chemistry and capacitive behaviors of porous carbon electrode," *Electrochimica Acta*, vol. 266, pp. 420–30, 2018.

[148] P. Du, L. Liu, Y. Dong et al., "Synthesis of hierarchically porous boron-doped carbon material with enhanced surface hydrophobicity and porosity for improved supercapacitor performance," *Electrochimica Acta*, vol. 370, Article ID 137801, 2021.

[149] X. Lian, Z. Sun, Q. Mei et al., "Biomass template derived boron/oxygen co-doped carbon particles as advanced anodes for potassium-ion batteries," *Energy & Environmental Materials*, vol. 5, no. 1, pp. 344–52, 2022.

[150] S. Kumar, G. Saeed, L. Zhu, K. N. Hui, N. H. Kim, and J. H. Lee, "0D to 3D carbon-based networks combined with pseudocapacitive electrode material for high energy density supercapacitor: A review," *Chemical Engineering Journal*, vol. 403, Article ID 126352, 2021.

[151] S. Rawal, Y. Kumar, U. Mandal, A. Kumar, R. Tanwar, and B. Joshi, "Synthesis and electrochemical study of phosphorus-doped porous carbon for supercapacitor applications," *SN Applied Sciences*, vol. 3, no. 2, pp. 141–14, 2021.

[152] K. Dujearic-Stephane, M. Gupta, A. Kumar et al., "The effect of modifications of activated carbon materials on the capacitive performance: surface, microstructure, and wettability," *Journal of Composites Science*, vol. 5, no. 3, p. 66, 2021.

[153] R. Liu, J.-X. Wang, and W.-D. Yang, "Hierarchical porous heteroatoms—co-doped activated carbon synthesized from coconut shell and its application for supercapacitors," *Nanomaterials*, vol. 12, no. 19, p. 3504, 2022.

[154] B. G. Salas-Enríquez, A. M. Torres-Huerta, E. Conde-Barajas, M. A. Domínguez-Crespo, L. Díaz-García, and M. Negrete-Rodríguez, "Activated carbon production from the Guadua amplexifolia using a combination of physical and chemical activation," *Journal of Thermal Analysis and Calorimetry*, vol. 124, no. 3, pp. 1383–98, 2016.

[155] J. Pallarés, A. González-Cencerrado, and I. Arauzo, "Production and characterization of activated carbon from barley straw by physical activation with carbon dioxide and steam," *Biomass and Bioenergy*, vol. 115, pp. 64–73, 2018.

[156] M. Shoaib and H. M. Al-Swaidan, "Optimization and characterization of sliced activated carbon prepared from date palm tree fronds by physical activation," *Biomass and Bioenergy*, vol. 73, pp. 124–34, 2015.

[157] A. Barroso-Bogeat, M. Alexandre-Franco, C. Fernández-González, A. Macías-García, and

V. Gómez-Serrano, "Temperature dependence of the electrical conductivity of activated carbons prepared from vine shoots by physical and chemical activation methods," *Microporous and Mesoporous Materials*, vol. 209, pp. 90–8, 2015.

[158] N. T. Mai, M. N. Nguyen, T. Tsubota, P. L. Nguyen, and N. H. Nguyen, "Evolution of physico-chemical properties of Dicranopteris linearis-derived activated carbon under various physical activation atmospheres," *Scientific Reports*, vol. 11, no. 1, Article ID 14430, 2021.

[159] A. Fombona-Pascual, N. Díez, A. B. Fuertes, and M. Sevilla, "Eco-friendly synthesis of 3D disordered carbon materials for high-performance dual carbon na-ion capacitors," *ChemSusChem*, vol. 15, no. 19, Article ID e202201046, 2022.

[160] N. Talreja, S. Jung, L. T. H. Yen, and T. Kim, "Phenol-formaldehyde-resin-based activated carbons with controlled pore size distribution for high-performance supercapacitors," *Chemical Engineering Journal*, vol. 379, Article ID 122332, 2020.

[161] S. Yang, S. Wang, X. Liu, and L. Li, "Biomass derived interconnected hierarchical micro-meso-macro- porous carbon with ultrahigh capacitance for supercapacitors," *Carbon*, vol. 147, pp. 540–9, 2019.

[162] Q. Zhang, K. Han, S. Li, M. Li, J. Li, and K. Ren, "Synthesis of garlic skin-derived 3D hierarchical porous carbon for high-performance supercapacitors," *Nanoscale*, vol. 10, no. 5, pp. 2427–37, 2018.

[163] S. Li, X. Tan, H. Li et al., "Investigation on pore structure regulation of activated carbon derived from sargassum and its application in supercapacitor," *Scientific Reports*, vol. 12, no. 1, pp. 10106–17, 2022.

[164] J. Wu, M. Xia, X. Zhang et al., "Hierarchical porous carbon derived from wood tar using crab as the template: performance on supercapacitor," *Journal of Power Sources*, vol. 455, Article ID 227982, 2020.

[165] Z. Zapata-Benabithe, C. D. Castro, and G. Quintana, "Kraft lignin as a raw material of activated carbon for supercapacitor electrodes," *Journal of Materials Science: Materials in Electronics*, vol. 33, no. 9, pp. 7031–47, 2022.

[166] M. A. Yahya, Z. Al-Qodah, and C. Z. Ngah, "Agricultural bio-waste materials as potential sustainable precursors used for activated carbon production: A review," *Renewable and Sustainable Energy Reviews*, vol. 46, pp. 218–35, 2015.

[167] D. Momodu, N. F. Sylla, B. Mutuma et al., "Stable ionic-liquid-based symmetric supercapacitors from capsicum seed-porous carbons," *Journal of Electroanalytical Chemistry*, vol. 838, pp. 119–28, 2019.

[168] L.-H. Zheng, M.-H. Chen, S.-X. Liang, and Q.-F. Lü, "Oxygen-rich hierarchical porous carbon derived from biomass waste-kapok flower for supercapacitor electrode," *Diamond and Related Materials*, vol. 113, Article ID 108267, 2021.

[169] J. Phiri, J. Dou, T. Vuorinen, P. A. Gane, and T. C Maloney, "Highly porous willow wood-derived activated carbon for high-performance supercapacitor electrodes," *ACS Omega*, vol. 4, no. 19, pp. 18108–17, 2019.

[170] P. Merin, P. Jimmy Joy, M. Muralidharan, E. Veena Gopalan, and A. Seema, "Biomass-derived activated carbon for high-performance supercapacitor electrode applications," *Chemical Engineering & Technology*, vol. 44, no. 5, pp. 844–51, 2021.

[171] U. W. Lee, G. Yang, and S. J. Park, "Improvement of mesoporosity on supercapacitive performance of activated carbons derived from coffee grounds," *Bulletin of the Korean Chemical Society*, vol. 42, no. 5, pp. 748–55, 2021.

[172] M. Liu, X. Yang, X. Wu et al., "Understanding the pore-structure dependence of supercapacitive performance for microporous carbon in aqueous KOH and H_2SO_4 electrolytes," *Electrochimica Acta*, vol. 401, Article ID 139422, 2022.

[173] B. Jiang, L. Cao, Q. Yuan et al., "Biomass straw-derived porous carbon synthesized for supercapacitor by ball milling," *Materials*, vol. 15, no. 3, p. 924, 2022.

[174] B. Pal, A. Yasin, V. Sunil, Z. Sofer, C.-C. Yang, and R. Jose, "Enhancing the materials circularity: from laboratory waste to electrochemical capacitors," *Materials Today Sustainability*, vol. 20, Article ID 100221, 2022.

[175] T. Eguchi, D. Tashima, M. Fukuma, and S. Kumagai, "Activated carbon derived from Japanese distilled liquor waste: Application as the electrode active material of electric double-layer capacitors," *Journal of Cleaner Production*, vol. 259, Article ID 120822, 2020.

[176] X. Xie, B. Zhang, Q. Wang et al., "Efficient microwave absorber and supercapacitors derived from puffed-rice-based biomass carbon: Effects of activating temperature," *Journal of Colloid and Interface Science*, vol. 594, pp. 290–303, 2021.

[177] E. Taer, R. Taslim, A. Putri, A. Apriwandi, and A. Agustino, "Activated carbon electrode made from coconut husk waste for supercapacitor application," *International Journal of Electrochemical Science*, vol. 13, no. 12, pp. 12072–84, 2018.

[178] A. R. Selvaraj, A. Muthusamy, C. Inho, H.-J. Kim, K. Senthil, and K. Prabakar, "Ultrahigh surface area biomass derived 3D hierarchical porous carbon nanosheet electrodes for high energy density supercapacitors," *Carbon*, vol. 174, pp. 463–74, 2021.

[179] Y. Chen, X. Xu, R. Ma et al., "Preparation of hierarchical porous carbon by pyrolyzing sargassum under microwave: The internal connection between structure–oriented regulation and performance optimization of supercapacitors," *Journal of Energy Storage*, vol. 53, Article ID 105190, 2022.

[180] B. Liu, Y. Liu, H. Chen, M. Yang, and H. Li, "Oxygen and nitrogen co-doped porous carbon nanosheets derived from Perilla frutescens for high volumetric performance supercapacitors," *Journal of Power Sources*, vol. 341, pp. 309–17, 2017.

[181] M. J. Mostazo-López, R. Ruiz-Rosas, E. Morallón, and D. Cazorla-Amorós, "Generation of nitrogen functionalities on activated carbons by amidation reactions and Hofmann rearrangement: Chemical and electrochemical characterization," *Carbon*, vol. 91, pp. 252–65, 2015.

[182] D. Salinas-Torres, S. Shiraishi, E. Morallón, and D. Cazorla-Amorós, "Improvement of carbon materials performance by nitrogen functional groups in electrochemical capacitors in organic electrolyte at severe conditions," *Carbon*, vol. 82, pp. 205–13, 2015.

[183] D. Salinas-Torres, R. Ruiz-Rosas, E. Morallón, and D. Cazorla-Amorós, "Strategies to enhance the performance of electrochemical capacitors based on carbon materials," *Frontiers in Materials*, vol. 6, 2019.

[184] C. Pan, X. Fu, W. Lu et al., "Effects of conductive carbon materials on dry anaerobic digestion of sewage sludge: process and mechanism," *Journal of Hazardous Materials*, vol. 384, Article ID 121339, 2020.

[185] B. Huang, Y. Liu, and Z. Xie, "Two dimensional nanocarbons from biomass and biological molecules: Synthetic strategies and energy related applications," *Journal of Energy Chemistry*, vol. 54, pp. 795–814, 2021.

[186] B. Yan, J. Zheng, L. Feng et al., "Wood-derived biochar as thick electrodes for high-rate performance supercapacitors," *Biochar*, vol. 4, no. 1, p. 50, 2022.

[187] H. Yamada, H. Nakamura, F. Nakahara, I. Moriguchi, and T. Kudo, "Electrochemical Study of High Electrochemical Double Layer Capacitance of Ordered Porous Carbons with Both Meso/Macropores and Micropores," *The Journal of Physical Chemistry C*, vol. 111, no. 1, pp. 227–33, 2006.

[188] E. Dhandapani, S. Thangarasu, S. Ramesh, K. Ramesh, R. Vasudevan, and N. Duraisamy, "Recent development and prospective of carbonaceous material, conducting polymer and their composite electrode materials for supercapacitor—A review," *Journal of Energy Storage*, vol. 52, Article ID 104937, 2022.

[189] A. Fagan-Murphy, S. Kataria, and B. A. Patel, "Electrochemical performance of multi-walled carbon nanotube composite electrodes is enhanced with larger diameters and reduced specific surface area," *Journal of Solid State Electrochemistry*, vol. 20, no. 3, pp. 785–92, 2016.

[190] J. Xiao, J. Han, C. Zhang, G. Ling, F. Kang, and Q. H. Yang, "Dimensionality, function and performance of carbon materials in energy storage devices," *Advanced Energy Materials*, vol. 12, no. 4, Article ID 2100775, 2022.

[191] H. H. Phan and A. N. Phan, "Carbon nanostructures with the ultra-high surface area and porosity derived from biomass," *Green Energy and Technology*, vol. 4, pp. 99–125, 2023.

[192] M. Usha Rani, K. Nanaji, T. N. Rao, and A. S. Deshpande, "Corn husk derived activated carbon with enhanced electrochemical performance for high-voltage supercapacitors," *Journal of Power Sources*, vol. 471, Article ID 228387, 2020.

[193] G. Zhang, Y. Chen, Y. Chen, and H. Guo, "Activated biomass carbon made from bamboo as electrode material for supercapacitors," *Materials Research Bulletin*, vol. 102, pp. 391–8, 2018.

[194] A. C. Ngandjong, T. Lombardo, E. N. Primo et al., "Investigating electrode calendering and its impact on electrochemical performance by means of a new discrete element method model: Towards a digital twin of Li-Ion battery manufacturing," *Journal of Power Sources*, vol. 485, Article ID 229320, 2021.

[195] L. Zhang, X. Yang, F. Zhang et al., "Controlling the effective surface area and pore size distribution of sp2 carbon materials and their impact on the capacitance performance of these materials," *Journal of the American Chemical Society*, vol. 135, no. 15, pp. 5921–9, 2013.

[196] O. Barbieri, M. Hahn, A. Herzog, and R. Kötz, "Capacitance limits of high surface area activated carbons for double layer capacitors," *Carbon*, vol. 43, no. 6, pp. 1303–10, 2005.

[197] Y. Jin, K. Tian, L. Wei, X. Zhang, and X. Guo, "Hierarchical porous microspheres of activated carbon with a high surface area from spores for electrochemical double-layer capacitors," *Journal of Materials Chemistry A*, vol. 4, no. 41, pp. 15968–79, 2016.

[198] Y. Wang, Y. Chen, H. Zhao et al., "Biomass-derived porous carbon with a good balance between high specific surface area and mesopore volume for supercapacitors," *Nanomaterials*, vol. 12, no. 21, p. 3804, 2022.

[199] M. Amiri and F. Golmohammadi, "Biomass derived hierarchical 3D graphene framework for high performance energy storage devices," *Journal of Electroanalytical Chemistry*, vol. 849, Article ID 113388, 2019.

[200] X. Qu, Y. Liu, C. Zhang et al., "Effect of different pretreatment methods on sesame husk-based activated carbon for supercapacitors with aqueous and organic electrolytes," *Journal of Materials Science: Materials in Electronics*, vol. 30, no. 8, pp. 7873–82, 2019.

[201] H. Quan, X. Fan, W. Wang, W. Gao, Y. Dong, and D. Chen, "Hierarchically porous carbon derived from biomass: Effect of mesopore and heteroatom-doping on electrochemical performance," *Applied Surface Science*, vol. 460, pp. 8–16, 2018.

[202] D. Li, Y. Huang, C. Yu, C. Tang, and J. Lin, "Rapid synthesis of biomass-derived carbon via induction pyrolysis for supercapacitors," *Diamond and Related Materials*, vol. 136, Article ID 109956, 2023.

[203] P. Hao, Z. Zhao, J. Tian et al., "Hierarchical porous carbon aerogel derived from bagasse for high performance supercapacitor electrode," *Nanoscale*, vol. 6, no. 20, pp. 12120–9, 2014.

[204] W. Chen, X. Wang, M. Feizbakhshan et al., "Preparation of lignin-based porous carbon with hierarchical oxygen-enriched structure for high-performance supercapacitors," *Journal of Colloid and Interface Science*, vol. 540, pp. 524–34, 2019.

[205] I. I. G. Inal, S. M. Holmes, A. Banford, and Z. Aktas, "The performance of supercapacitor electrodes developed from chemically activated carbon produced from waste tea," *Applied Surface Science*, vol. 357, pp. 696–703, 2015.

[206] C.-L. Yeh, H.-C. Hsi, K.-C. Li, and C.-H. Hou, "Improved performance in capacitive deionization of activated carbon electrodes with a tunable mesopore and micropore ratio," *Desalination*, vol. 367, pp. 60–8, 2015.

[207] D. Liu, W. Zhang, and W. Huang, "Effect of removing silica in rice husk for the preparation of activated carbon for supercapacitor applications," *Chinese Chemical Letters*, vol. 30, no. 6, pp. 1315–9, 2019.

[208] F. Ma, S. Ding, H. Ren, and Y. Liu, "Sakura-based activated carbon preparation and its performance in supercapacitor applications," *RSC Advances*, vol. 9, no. 5, pp. 2474–83, 2019.

[209] S. Li, K. Han, P. Si, J. Li, and C. Lu, "High-performance activated carbons prepared by KOH activation of gulfweed for supercapacitors," *International Journal of Electrochemical Science*, vol. 13, no. 2, pp. 1728–43, 2018.

[210] G. Dai, L. Zhang, Y. Liao et al., "Multi-scale model for describing the effect of pore structure on carbon-based electric double layer," *The Journal of Physical Chemistry C*, vol. 124, no. 7, pp. 3952–61, 2020.

[211] C. Kim, C. Zhu, Y. Aoki, and H. Habazaki, "Heteroatom-doped porous carbon with tunable pore structure and high specific surface area for high performance supercapacitors," *Electrochimica Acta*, vol. 314, pp. 173–87, 2019.

[212] Y. M. Lian, M. Ni, L. Zhou, R. J. Chen, and W. Yang, "Synthesis of biomass-derived carbon induced by cellular respiration in yeast for supercapacitor applications," *Chemistry–A European Journal*, vol. 24, no. 68, pp. 18068–74, 2018.

[213] M. Wu, S. Xu, X. Li et al., "Pore regulation of wood-derived hierarchical porous carbon for improving electrochemical performance," *Journal of Energy Storage*, vol. 40, Article ID 102663, 2021.

[214] L. Hu, J. W. Choi, Y. Yang et al., "Highly conductive paper for energy-storage devices," *Proceedings of the National Academy of Sciences*, vol. 106, no. 51, pp. 21490–4, 2009.

[215] S. Lehtimäki, A. Railanmaa, J. Keskinen, M. Kujala, S. Tuukkanen, and D. Lupo, "Performance, stability and operation voltage optimization of screen-printed aqueous supercapacitors," *Scientific Reports*, vol. 7, no. 1, Article ID 46001, 2017.

[216] L. Liu, H. Zhao, and Y. Lei, "Advances on three-dimensional electrodes for micro-supercapacitors: A mini-review," *InfoMat*, vol. 1, no. 1, pp. 74–84, 2019.
[217] Y. Gogotsi and P. Simon, "True performance metrics in electrochemical energy storage," *Science*, vol. 334, no. 6058, pp. 917–8, 2011.
[218] Z. Pan, H. Zhi, Y. Qiu et al., "Achieving commercial-level mass loading in ternary-doped holey graphene hydrogel electrodes for ultrahigh energy density supercapacitors," *Nano Energy*, vol. 46, pp. 266–76, 2018.
[219] Y. Xu, Z. Lin, X. Huang, Y. Liu, Y. Huang, and X. Duan, "Flexible solid-state supercapacitors based on three-dimensional graphene hydrogel films," *ACS Nano Journal*, vol. 7, no. 5, pp. 4042–9, 2013.
[220] H. Li, Y. Tao, X. Zheng et al., "Ultra-thick graphene bulk supercapacitor electrodes for compact energy storage," *Energy & Environmental Science.*, vol. 9, no. 10, pp. 3135–42, 2016.
[221] S. Kumagai, K. Mukaiyachi, and D. Tashima, "Rate and cycle performances of supercapacitors with different electrode thickness using non-aqueous electrolyte," *Journal of Energy Storage*, vol. 3, pp. 10–7, 2015.